Investigation into the effect of LRRK2-Rab10 protein interactions on the Proboscis Extension Response of the fruit fly *Drosophila melanogaster*

Laura Covill

Masters by Research

University of York

Biology

December 2018

Abstract

Parkinson's Disease (PD) is a debilitating disease which affects 1% of the population worldwide and is characterised by stiffness, tremor and bradykinesia. PD is a complex disease with many suspected genetic and environmental causes, and it is critical to understand all the pathways involved in disease progression to develop effective therapies for PD, which currently has no cure. A kinase-coding gene, *LRRK2* has emerged as a focal point for much PD research, particularly PD-associated SNP *LRRK2-G2019S*, which leads to LRRK2 overactivity. Rab proteins, a series of small GTPases, have been identified among the proteins phosphorylated by LRRK2. These interactions may be modelled in the fruit fly *Drosophila melanogaster*.

Using optogenetics in the fly, this project investigates the relationship between the LRRK2-G2019S and Rab10 interaction, and the speed and degree of tremor of Proboscis Extension Response (PER) by triggering a PER in fly lines of different genotypes. Significant bradykinesia in Rab10 null flies which was not recreated in flies with dopaminergic neuron $Rab10^{RNAi}$ suggests that the bradykinesia PER phenotype is caused by off-target effect of *Rab10*-KO in another tissue of the fly than the dopaminergic neurons. Over-expression of *Rab10* in dopaminergic neurons of flies also expressing *LRRK2-G2019S* produced resting tremor and inability to fully extend the proboscis.

Contents

List of Tables

List of Figures

List of Accompanying Material

Youtube videos

PER of Gr5aLexA::LexAopReaChR fly
https://www.youtube.com/watch?v=Zy4qGGrn1ro&feature=youtu.be

PER of UAS-Rab10;Gr5aLexA::LexAopReaChR;TH::G2019S fly
https://www.youtube.com/watch?v=_0cHnyNpRTg

GitHub PER video analysis code

https://github.com/lcovill/fruit-flies-analysis-software/blob/master/core.clj

Acknowledgements

Many thanks go to my supervisor, Dr Chris Elliott, whose direction, insight and patience have been inspiring. My thanks also to many others who have spared their time and energy to give help and advice: my co-supervisor, Dr Sean Sweeney; Dr Gareth Evans, who kindly participated in my thesis advisory panel; Dr Laurence Wilson for analysis of the proboscis extension tremor; Professor Dario Alessi; Dr Robin Hiesinger and his lab for the Rab10 knockout flies; the Elliott lab, Khalid Jambi and Alison Fellgett; the Sweeney lab, Dr Ryan West, Dr Chris Ugbode, Dr Nathan Garnham, and Laura Fort; Katy Hyde; Dr Iain Hartnell, Alex Haworth, Grace Cowen, Annie Smith, Dr Nick Johnson and Dr Jane Pennifold; Dr Jack Munns, who gave font advice; and thanks as always to Daniel Gullberg and to my family, who continue to endeavour to know what I am talking about.

Declaration

I declare that this thesis is a presentation of original work and I am the sole author. This work has not previously been presented for an award at this, or any other, University. All sources are acknowledged as References. Some data and analysis presented in this work appears in the poster https://pure.york.ac.uk/portal/en/publications/interaction-of-lrrk2g2019s-with-rab-gtpases-in-vivo(07a7bbde-4bbb-465a-8a66-c48db6d8b988).html, displayed at the 2018 Biennial International LRRK2 Meeting of the Biochemical Society, Padua, and in the preprint https://www.biorxiv.org/content/10.1101/586073v1 (Petridi et al., 2019).

Introduction

1.1 Parkinson's Disease

1.1.1 Phenotype of Parkinson's Disease

Parkinson's Disease is a neurodegenerative disorder found in approximately 1% of the population worldwide (de Lau and Breteler, 2006). It is diagnosed by the presence of two out of three of key symptoms: bradykinesia, tremor in hands and arms which later spreads to legs and feet, and muscle rigidity. However, the defining characteristic of Parkinson's by which it is differentiated from other similar neurodegenerative disorders is the progressive loss of dopamine-containing neurons, and responsiveness of the condition to L-Dopa. Conclusive diagnosis may be challenging due to the neuron loss being identifiable only post-mortem (Jankovic, 2008). Other symptoms may include loss of balance, and various non-motor symptoms, such as worsening eyesight (Armstrong, 2008) and depression (Marsh, 2013).

Beyond discernible physical symptoms, the principle manifestation of PD at the cellular level is the presence of Lewy bodies, toxic aggregates composed principally of alpha-synuclein (Spillantini et al., 1997). Other proteins which may appear in Lewy bodies include ubiquitin and tau proteins, and as with tauopathies the Lewy bodies may be associated with neurofibrillary tangles (Zhang et al., 2018). Alpha-synuclein is an intrinsically disordered protein which is soluble in the cytosol as a monomer. However, exposure to hydrophobic molecules or environment can cause the centre of the protein to fold into beta sheets, which may dimerise or form aggregates. One misfolded alpha-synuclein protein may influence other alpha-synuclein proteins to fold the same way in order to interact with them and create a global free energy minimum (Ulmer et al., 2005). Lewy bodies are extremely detrimental to the cell architecture and trafficking, disrupting organelles and contributing to degradation of mitochondria and the cell nucleus. Cell death releases Lewy bodies into the brain tissue, where they may be taken up by other cells. The prion-like effect of the misfolded alpha-

synuclein can therefore be spread through the substantia nigra, the area of the brain where Lewy bodies are commonly found in PD (Power et al., 2017). Nine clusters of dopaminergic neurons are found in the mammalian brain. 95% of these dopaminergic neurons are represented in the substantia nigra region of the brain, where they comprise 3-5% of the cells. They are responsible for control of voluntary movement, and dopaminergic neurons found elsewhere are also involved in regulating a number of disparate behaviours including motivation and reward (Chinta and Andersen, 2005), achieved by projecting into other regions of the brain. Several features distinguish dopaminergic neurons from other types of neuron, notably the presence of the enzyme tyrosine hydroxylase, responsible for conversion of tyrosine into L-Dopa, a precursor molecule for dopamine. L-Dopa is decarboxylated to complete dopamine production. Tyrosine hydroxylase is coded for by gene *TH*, which is highly conserved between species; the homologue in *Drosophila melanogaster* is *Pale*, with a central coding domain containing 80.5% sequence identity. Deleterious mutations in TH cause Segawa syndrome, which manifests Parkinsonian features and responds to L-Dopa (Goswami et al., 2017).

1.1.2 Genetics of Parkinson's Disease

PD is a complex disorder with variability regarding type and severity of phenotype, age of onset, and genetic aetiology. Several mutations in candidate genes have been discovered in families causing versions of Parkinson's with an earlier age of onset than average, and may also cause faster neurodegeneration (Houlden and Singleton, 2012). Principally this has revolved around alpha-synuclein (Singleton et al., 2003, Polymeropoulos et al., 1997). Mutations or CNVs in the region of *SNCA*, the gene coding for alpha-synuclein, have been found to increase incidence of alpha-synuclein aggregation. The rarity of *SNCA* mutations, with only three deleterious mutations reported in families (Kruger et al., 1998, Zarranz et al., 2004) and lack of these mutations in the general population, is evidence for the scale of damage to the cells which may be caused by any alteration in the structure and concentration of alpha-synuclein. Other candidate genes for PD often code for proteins involved in intracellular membrane trafficking, such as *LRRK2* (leucine rich repeat kinase 2),

MAPT, *GBA*, and *VPS35* (Reed et al., 2018). Mutations in *MAPT* (microtubule-associated protein tau) causing Parkinsonism is not thought to be associated with development of Lewy bodies or alpha-synuclein abnormalities, but further suggests a critical role for the cytoskeleton and transport within the cell in the search for genetic causes and therapies for PD (Wray and Lewis, 2010). Meanwhile, genome-wide association studies (GWAS) have indicated multiple small effect alleles that may increase susceptibility to environmental factors in the general population, or interact with each other to produce a larger effect size. Indeed, GWAS indicates that LRRK2 is a risk factor for PD. However, no high-risk common alleles for PD have been discovered (Fung et al., 2006, Maraganore et al., 2006). Much of ongoing PD research has focused on identifying interaction maps for the protein products of genes with known PD association. Overall, mutations in/near *LRRK2* are the most common genetic cause of PD. These include the amino acid substitutions *G2019S* and *I2020T*.

In order to understand more about the link between *LRRK2* mutation and neurodegeneration, a number of labs have created transgenic rodent models using *LRRK2* manipulations. These have been inconsistent, and do not reliably recapitulate the PD phenotypes (Beal, 2010). This may be because they do not make the neuromelanin which gives the *substantia nigra* its dark colour (Barden and Levine, 1983, Marsden, 1961), or due to differences in dopamine metabolism between humans and rodents (Burbulla et al., 2017). However, fly models of PD have been successfully exploited as a model of PD (Whitworth, 2011).

1.2 *Drosophila* as a model organism

1.2.1 Analysis of *Drosophila* as a model organism for PD

Drosophila melanogaster has emerged as a standout model organism in which to model PD and other neurodegenerative diseases due to several unique aspects. It has a genome which has been highly characterized over decades of study, and which contains homologs of 75% of human disease loci (Reiter et al., 2001). The wide scale of effect size seen in humans may be easily mimicked in *Drosophila*. *Drosophila* also has a short generation span permitting faster crosses than mammalian

models, and several powerful genetic tools are available in *Drosophila* making complex research possible.

They are easy to store and maintain, and allow for large scale, high-throughput projects which would not be possible with a larger and more complex organism, such as mice. An additional advantage when studying neurodegenerative disease is the shorter time until onset of symptoms due to the shorter lifespan of *Drosophila*. Modelled in rodents, it is possible that two years could be necessary to see the same PD symptoms which are present in *Drosophila* after 28 days (Cording et al., 2017, Dawson et al., 2010). Yeast has often been used to observe the biochemistry of protein aggregates commonly found in neurodegenerative disease, however when considering the effects on an entire complex system, *Drosophila* is an ideal model organism to use for Parkinson's Disease due to the segmented brain and high visual capacity (Cauchi and van den Heuvel, 2006). The simplicity of the fly brain makes it easier to work with, although it may also prevent the fly from being a good model for a human brain when more complex functions are involved in a disease.

Drosophila brains consist of 135,000 neurons, surrounded by glial cells. The brain is divided into two mushroom body structures projecting out from a central complex. Mushroom bodies, common in insects and arthropods, are packed cell somata which form three distinct lobes. 15 dopaminergic neuron clusters have been identified in flies, increasing from 9 in humans. These clusters project into multiple different regions of the fly brain, which is consistent with the wide-ranging activities which dopaminergic neurons are responsible for (Hartenstein et al., 2017). Many aspects of the fly brain morphology are extremely different from the human brain. However, processes in and between dopaminergic neurons are well-conserved between humans and flies at a molecular level, and share many of the same functions. The earlier described process of dopamine synthesis involving TH is conserved between humans and *Drosophila*, and *Drosophila* dopaminergic neurons are responsible for control of voluntary movement and reward behaviours as in humans, allowing the use of *Drosophila* as a model for human diseases of dopaminergic neurons.

Many of the most detrimental problems seen in Parkinson's disease are also seen in fly models: bradykinesia (slowed movement), akinesia (difficulty initiating movement), tremor, and loss of dopaminergic neurons (Whitworth, 2011, Cording et al., 2017).

When using *Drosophila* as a model organism, it must also be noted that the model has several disadvantages. Lack of a blood-brain barrier prevents precise modelling of drug delivery; therefore validation of any pharmaceutical trials must be validated in organisms which have a similar delivery system to humans.

1.2.2 The genetics of *Drosophila*

Drosophila melanogaster have four pairs of chromosomes. Chr4 is extremely small and the majority of work in *Drosophila* genetics is therefore performed using only the first three. These chromosomes have the advantage of well-established balancer chromosomes, which are used when deleterious mutations, or disadvantageous transgenic fly lines need to be maintained. These prevent the desired mutation from being lost from the population, and also to prevent alleles of interest on the same chromosome being separated by recombination. Balancer chromosome homozygosity is lethal, but flies which carry a heterozygous mutation and balancer chromosome can be identified by the dominant marker or markers found on the balancer chromosome. Balancer chromosomes are available for each chromosome: *FM7* causes a bar eye phenotype and is a balancer chromosome for chromosome 1, *CyO* causes curly wings and is a balancer chromosome for chromosome 2, and *TM6B* causes extra bristles on the thorax and is a balancer chromosome for chromosome 3.

1.2.3 Gal4-UAS system

The UAS-Gal4 system is part of the *Drosophila* genetic toolkit (Brand and Perrimon, 1993). It is a binary expression system, using genes originally discovered in yeast, but not present in the fly (Figure 1A). A transgene is created by inserting the transcriptional activator *Gal4* along with a characterised driver or promotor gene into the fly genome. The promotor then determines which cells will express Gal4. Where the driver is transcribed, Gal4 will also be expressed, while in all other

cells where the driver is silenced, the Gal4 protein will not exist as *Gal4* is not normally present in the *Drosophila* genome. The expression of Gal4 has no effect on normal *Drosophila* cells, but when the upstream activating sequence (*UAS*) is also present in the genome, Gal4 will bind and activate transcription of the gene immediately downstream of the *UAS*. Thus to complete the system, a second transgene can be created of the UAS sequence, and a target or reporter gene immediately following it. A normal technique to generate a fly line containing both transgenes is to cross a fly with promotor-Gal4, where the promotor is expressed in the specific cells of interest e.g. neurons, with a fly with UAS-target, resulting in offspring with both genes. Thousands of fly lines have been created using Gal4 or UAS transgenes, which can be crossed to create desirable combinations of gene to be expressed, and the location it is to be expressed in.

Here we deployed the GAL4-UAS system to express the Parkinson's disease related gene, *LRRK2*, in the dopaminergic neurons. This leads to a number of phenotypes, both motor (Cording et al., 2017), and non-motor (Hindle et al., 2013), so replicating the human disease. Notably, dopaminergic expression of the *G2019S* and *I2020T* forms of LRRK2 results in a slower proboscis extension response (Cording et al., 2017), due to the action of the mutant protein in a single dopaminergic neuron, the TH-VUM (Marella et al., 2012).

One of the problems noted with sucrose stimulation of the Proboscis Extension Response was variability in the operator's application of the sucrose droplet to the legs. The experimental approach could be much improved by a more defined and precise stimulus, here an optogenetic activation of the sucrose-sensing neurons. Although the collection of available UAS lines contains a number of possible light-activated ion channels (channelrhodopsins), these would not permit independent expression of LRRK2 and the channelrhodopsin (ChR). To circumvent this we turned to a second binary expression system, LexA-LexAop.

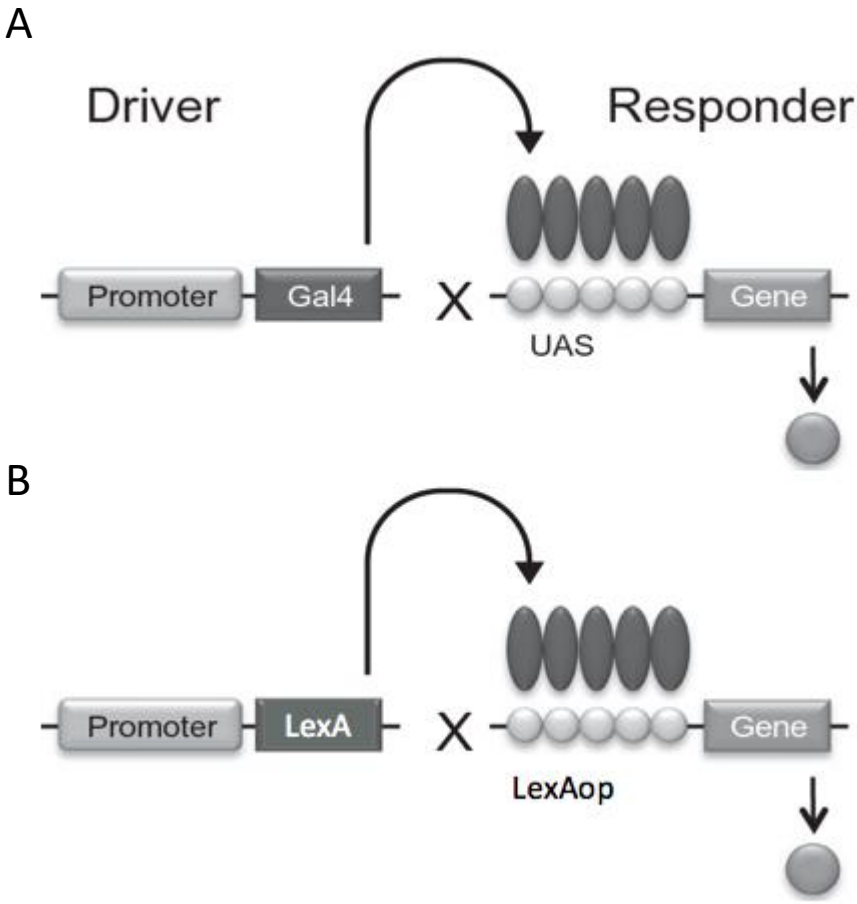

Figure 1. Two binary expression systems used in *Drosophila*. A. Gal4-UAS (Lynd and Lycett, 2011) **B.** LexA-LexAop. The two systems do not interfere with each other and can be used simultaneously.

1.2.4 LexA-LexAop system

The LexA-LexAop system is based on the same idea as the GAL4-UAS, a two component expression system. LexA is a bacterial transcription factor which, when it has been fused with a C-terminal activation domain from GAL4 or VP16 (Sadowski et al., 1988), drives transcription of any reporter gene with a LexAop sequence present in its promoter region for LexA to bind to (Figure 1B). Since the LexA-LexAop system uses a bacterial rather than a yeast transcription factor, it is completely separate to the UAS-Gal4 system, allowing them to be used as complementary systems to control targeted expression of different proteins in different cell types. Examples of applications of the two systems in duality include mosaic tissue analysis (Lai and Lee, 2006). The LexA-LexAop system has

been used to provoke desired behavioural responses in flies by driving ChRs to be expressed in neurons responsible for activating various behaviours (Inagaki et al., 2014).

Gr5a is the gene coding for Gustatory receptor 5a, found in sugar-activated chemosensory neurons on the fly's front legs (Dahanukar et al., 2007, Cording et al., 2017). Activation of the sugar neurons usually occurs when the fly has encountered food, and through a cascade of activations in the interneuronal pathway, contracts the M3 muscle and causes it to reach out its proboscis as a reflex (Cording et al., 2017). The entire signal from stimulus to beginning the proboscis extension is transmitted in a few milliseconds. *Gr5a* can be attached to *LexA* in the LexA-LexAop system, and thus when *Gr5a* is activated, Gr5aLexA will also drive transcription of the *LexAop* transgene, so that translation of the protein coded for by the gene recombined with *LexAop* will also be expressed in Gr5a-neurons.

ReaChR is a red-shifted variant of channel rhodopsin, a family of light-gated channels which selectively depolarise cells in which they are expressed when activated by the wavelength of light to which they are sensitive. Most ChRs are activated by light with wavelength of 450-545nm, wavelengths which may not penetrate deep into the brain due to being absorbed by common proteins. ReaChR is instead activated optimally by 627 nm (red), although 470-655 nm wavelengths have been employed with success. ReaChR is fully described by Lin et al, 2013. In *LexAop-ReaChR* flies, where the transgene *LexAopReaChR* is under the control of *LexAop*, ReaChR protein will only be expressed in the neurons with LexA. Crossing *Gr5a-LexA* and *LexAop-ReaChR* lines produces flies which express ReaChR channels in the membranes of sugar-activated chemosensory cells. Thus, activation of ReaChR channels by light will produce the same response as if the fly had encountered sugar, but the proboscis extension reflex will be immediately triggered in a temporally and spatially defined manner.

1.3 LRRK2

LRRK2 is an autosomal dominant gene encoding a large protein of 286kDa (Cook et al., 2017). Genome-wide linkage first identified the gene in a Japanese family with Parkinsonian symptoms (Funayama et al., 2002), and since then mutations occurring in *LRRK2* have been identified as contributing to 1-2% of PD cases and between 3% and 41% of familial Parkinson's occurrences (Kachergus et al., 2005, Lesage et al., 2005, Mata et al., 2005, Nichols et al., 2005). The protein LRRK2 contains several domains which perform different functions (Figure 2), notably including a serine-threonine kinase. The large number of domains capable of different protein interactions allows LRRK2 to interact with many different proteins, and thus it is capable of involvement in multiple distinct signalling pathways and activities within the cell.

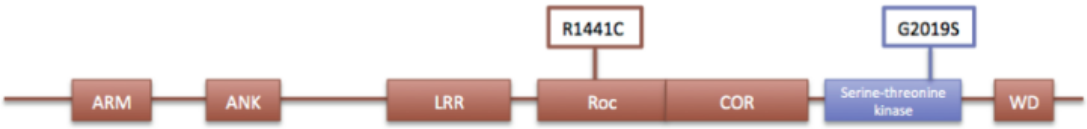

Figure 2. Map of LRRK2 domains. The positions of PD-associated SNPs R1441C and G2019S are also mapped. The ROC and kinase domains, which contain the majority of pathogenic SNPs, are the two domains with enzymatic activity. Created using Adobe Illustrator

LRRK2 can contain several different pathogenic SNPs which have been associated with late-onset PD, such as I2020T and G2019S (Healy et al., 2008b) in the kinase domain and R1441C/G (West et al., 2005) in the GTPase domain. Meanwhile, alpha-synuclein mutations are more associated with early-onset PD (Houlden and Singleton, 2012). Many of the PD-associated SNPs have been found to increase LRRK2 kinase activity. Differences in alpha-synuclein pathology between autopsied PD patients with known *LRRK2* mutations suggests that mechanisms of LRRK2 pathology are conducted at least partially separately to pathways increasing alpha-synuclein aggregation. G2019S, the most common LRRK2 mutation, increases kinase activity at least twofold, and I2020T and other LRRK2

mutations in the GTPase domain also increase kinase activity (West et al., 2005). However, incomplete penetrance is indicated, as extreme variance is seen in development and progression of PD, including whether the affected individual sufferer has Lewy bodies (Marti-Masso et al., 2009, Hasegawa et al., 2009).

Given the number of different pathways LRRK2 operates in, it is critical but non-trivial to discover all the putative mechanisms by which LRRK2 overactivity may contribute to dopaminergic neuron decay and development of Parkinsonian symptoms.

1.3.1 Interactions of LRRK2

LRRK2 has a role in endolysosomal trafficking and autophagy, two highly cooperative intracellular processes. Lysozymes have been shown to be missorted to lysosomes in LRRK2-KO mice due to the lack of Rab2a recruitment to the vesicles that would exocytose the lysozymes, resulting in susceptibility of the mice to listeria infection (Zhang et al., 2015). This may provide a link between LRRK2 mutations and the failure of PD dopaminergic neurons to remove Lewy Bodies. After alpha-synuclein and other proteins were sent to the lysosome for degradation, increased activity of LRRK2 caused hyper-phosphorylation of Rab proteins, which migrated to the lysosome membrane and initiated premature exocytosis of unfolded alpha-synuclein from the lysosome. These aggregates may then be engulfed by other cells in the substantia nigra. However, although co-localisation of alpha-synuclein and LRRK2 has been found (Guerreiro et al., 2013) and expressing LRRK2-G2019S in alpha-synuclein A53T mouse lines exacerbates degeneration of dopaminergic neurons (Lin et al., 2009, Daher et al., 2012), no direct evidence has been found to conclude whether these processes represent protein interactions or separate mechanisms.

It is suggested that LRRK2 phosphorylates Tau protein, either directly (Kawakami et al., 2012) or by mediating Tau phosphorylation by CDK5 (Shanley et al., 2015), causing its dissociation from microtubules necessary for dendrite growth and potentially contributing to the

hyperphosphorylated Tau aggregates known as neurofibrillary tangles. However, while many PD cases may contain both LRRK2 mutations, and Tau aggregates in some form (Ujiie et al., 2012), there are many further potential mechanisms yet to be examined.

The same *LRRK2* mutation may produce drastically different phenotypes, even within the same family. This reduced penetrance suggests that the mutated variants of this protein increase susceptibility to environmental or other genetic factors rather than directly impact disease progression. It has been established that the rate of *LRRK2-G2019S*-influenced neurodegeneration is increased by greater energy demands placed on neurons (Hindle et al., 2013).

Continued prevalence of deleterious SNPs in *LRRK2* within the population may be due to antagonistic pleiotropy. As PD onset typically occurs considerably later than reproductive years, advantageous effects being conveyed in early life, such as faster cognition and better eyesight (Himmelberg et al., 2018), would be experienced long before the debilitation of PD. In other instances, deleterious SNP-prevalence could be due to founder effect in particular populations such as the Berbers of North Africa (Lesage et al., 2005).

Due in part to the contribution of LRRK2 to both familial and non-familial PD, LRRK2 inhibitors are being investigated for therapeutics (Chan and Tan, 2017, Galatsis, 2017). With LRRK2 being considered as a target for treatment, it is even more crucial to discover the full pathway by which it is involved in development of PD. LRRK2 highly expressed in the brain, but is also found in high concentrations in the lungs and kidneys (Giasson et al., 2006). Concerns have been raised that lung and kidney toxicity may arise when LRRK2 inhibitors are used as PD treatment, as well as the potential for infections if the immune system role of LRRK2 is compromised (Baptista et al., 2013, Fuji et al., 2015). However, inhibiting a target protein downstream of LRRK2 in the same pathway could potentially avoid some or all of these issues.

Using a combination of data mining and protein microarray screening (embryonic kidney-based cell line), Tomkins et al., (2018) have developed a list of putative interaction partners of LRRK2. Experimentally, in the microarray screening, 78 proteins were found to interact with LRRK2, and though these have not all been verified *in vivo*, the implication is that LRRK2 is a non-specific kinase, capable of interacting with many proteins given co-localisation and the correct conditions.

Using mouse models with overactive LRRK2 protein, or a LRRK2 protein with normal activity but impervious to inhibition, Steger et al., (2016) were able to identify phosphopeptides which had been phosphorylated *in vivo* by LRRK2 and were therefore up- or down-regulated in the respective screens. The proteins were then determined by liquid chromatography-mass spectrometry, the techniques used together to give more robust results than previous studies where a single technique was employed. 14 Rab GTPases including Rab8A, Rab10, and Rab12, were found to be phosphorylated by LRRK2 on a conserved Thr residue in the Switch 2 domain. This experiment was the first to accurately determine only those kinase interactions which could occur *in vivo*, although it had the limitation that only proteins which LRRK2 phosphorylated would be identified, when LRRK2 is capable of interacting with other proteins in a myriad of other ways due to the multiple functional domains it possesses. However, it was noted that pathogenic LRRK2 mutations in the GTPase or WD-40 domains also increased the concentration of phosphorylated Rab8a and Rab10 *in vitro*.

1.3.2 Rab GTPases

Rab GTPases are small GTPases which regulate intracellular trafficking via the recruitment of effector proteins to aid vesicle creation, function, movement, and fusion (Eguchi et al., 2018, Pylypenko et al., 2018). There are 33 distinct Rab proteins in flies, and an estimated 70+ in humans, of which 23 fly proteins are direct homologues of human proteins. The basic structure of Rabs, which comparative to LRRK2 are small proteins of around 20-30 kDa (Pereira-Leal and Seabra, 2000), have a GTPase

domain of α-helices and β-sheets linked to an intrinsically disordered C-terminal sequence which is prenylated immediately after translation to allow membrane-embedding (Kiral et al., 2018). This disordered sequence likely determines which membrane the Rab is transported to after translation, and unlike the GTPase domain, it is not conserved between Rabs, or between species. The GTPase domain contains a nucleotide-binding P-loop, Switch 1, and Switch 2 (Figure 3).

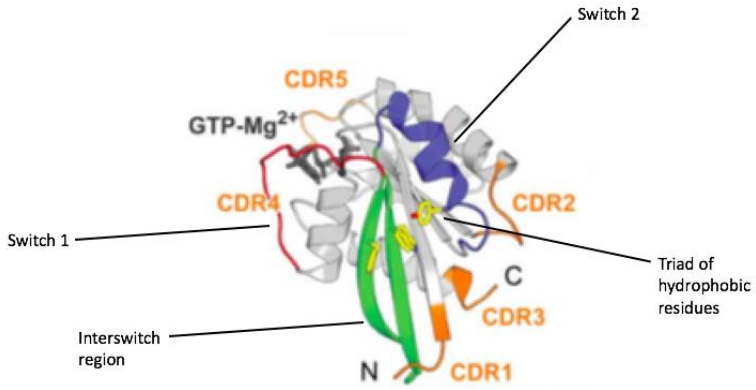

Figure 3. 3D structure of Rab3A (Pylypenko et al., 2017). Switch 1 (red) and Switch 2 (blue) are labelled. The phosphate group on Switch 2 interacts with the GTP third phosphate group. Complementarity determining regions (CDRs) are also labelled.

After a Rab has been inserted into the membrane of an organelle, vesicle, or cell, anchored by its geranylgeranyl lipid modification, it is active and able to recruit effector proteins when it is bound to GTP, and inactive when it is GDP-bound, thus functioning as a molecular switch (Zhen and Stenmark, 2015). Activation occurs when GDP is released and replaced with GTP, a slow process which must be catalysed by a Guanine nucleotide exchange factor (GEF). The GEF induces conformational change to the P-loop, Switch 1, and Switch 2 domains of the Rab protein with which it interacts, allowing the release of GDP. As with release of the GDP, GTP hydrolysis is a slow reaction requiring a catalyst. An arginine or glutamine residue present in (GAPs) interacts with the GTP-bound Rab, allowing it to maintain stability whilst releasing a phosphate group from GTP, hydrolysing to GDP (Vetter and Wittinghofer, 2001, Figure 4).

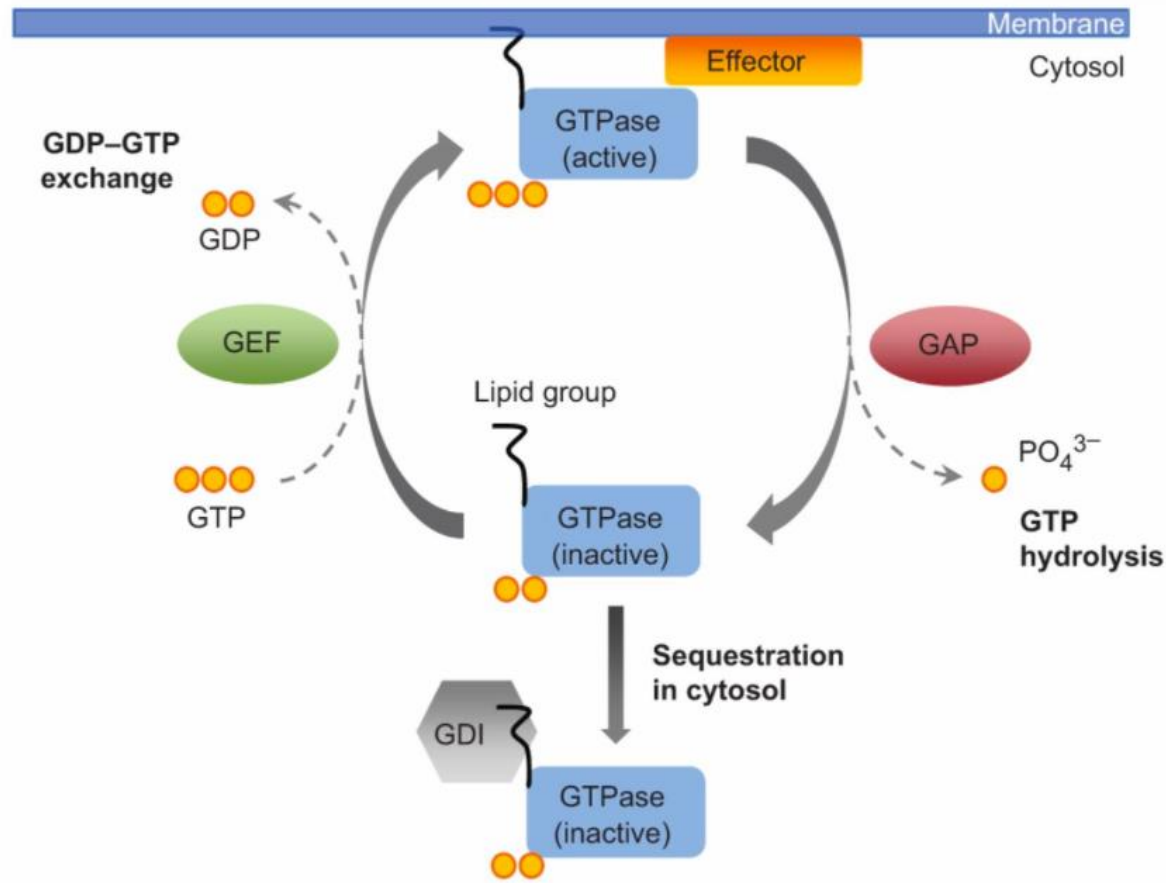

Figure 4. The life-cycle in the cell of a small GTPase protein, such as a Rab protein. (Bento et al., 2013)

When a Rab protein is being recycled from an acceptor membrane to a donor membrane, it is inactive in the cytosol, tightly bound to a guanosine nucleotide dissociation inhibitor (GDI). Although the full and precise mechanism by which a Rab protein may be extracted from the GDI which it is bound to in the cytosol is unknown, it is likely that phosphorylation by LRRK2 of the conserved residue in the Switch 2 region helps to facilitate this, as the GDI would be positioned closely to the Switch 2 region in the GDI-Rab complex, but cannot achieve this conformation after phosphorylation. Once the Rab protein has been extracted from this complex, possibly with the aid of a GDI-displacement factor (GDF) (Dirac-Svejstrup et al., 1997), it can be inserted into a donor membrane

and activated. However, Purlyte et al., (2018), suggest that GDIs are also necessary for delivery of Rab proteins to membranes.

Many proteins bind to non-phosphorylated Rabs preferentially other than GDIs. Rab geranyltransferase complex members (CHM, CHML, and RabGGTA/RabGGTB) are responsible for the prenylation of Rabs prior to their embedding in the target membrane. The Rab8a guanine nucleotide exchange factor Rabin8, which has been found to activate both Rab8a and Rab10 to promote neurite outgrowth (Homma and Fukuda, 2016), also has less activity interacting with Rabs when they have been phosphorylated (Steger et al, 2016), implying that GEFs generally may have less interaction with phosphorylated Rabs than non-phosphorylated Rabs.

Rabs have also been linked to neurodegeneration independently of LRRK2. Rab11 co-localises with alpha-synuclein, and is thought to interact with it (Chutna et al., 2014) and overexpression of Rab11 was able to partially rescue the effects of alpha-synuclein toxicity (Breda et al., 2015). Rab35 levels have been found to be increased in PD patient serum compared to healthy controls and neurodegenerative disease controls, and overexpression of Rab35 was found to cause neurodegeneration in mouse brains (Jeong et al., 2018). Rab35 is also phosphorylated by LRRK2, and Rab35 may positively regulate alpha-synuclein propagation (Bae et al., 2018). Several Rab proteins – Rab8A, Rab8B, and Rab13 – are substrates of PINK1, another PD-related protein (Lai et al., 2015).

1.3.3 LRRK2 interactions with Rab GTPases

Verification that LRRK2 directly phosphorylates Rab10 was performed has been performed (Steger et al., 2016). Rab10 and LRRK2 were incubated in a solution containing [γ-32P]ATP, before the products were separated on SDS-PAGE gels and digested with Trypsin. Identified phosphopeptides were analysed by LC-MS and the T73 residue in Rab10 was identified as the phosphorylation site by solid-phase Edman degradation. Further validation carried out in G2019S-expressing human embryonic kidney cells, where it was found that levels of P-T73-Rab10 decreased when a LRRK2-inhibitor was introduced. Sequence analysis on the 14 Rabs determined to be phosphorylated by

LRRK2 revealed that these are not the selection of Rabs with the highest sequence similarity, but rather a selection of different Rabs. It is therefore suggested that these are the Rabs which colocalise to the same areas of the cell as LRRK2 (Steger et al., 2017). Subsequent to this work, the Alessi lab also trialled use of Phos-tag acrylamide to assess Rab10 phosphorylation in a more high-throughput fashion by slowing process of tagged phosphorylated Rab10 through a gel, and reported that Rab10 phosphorylation was blocked when LRRK2 was knocked down (Ito et al., 2016), before identifying antibodies specific to T73-phosphorylated Rab10 (Lis et al., 2018). They suggest that quantification of phosphorylated Rab10, possibly in peripheral blood neutrophils, may be a useful tool in measuring the efficacy of LRRK2 inhibitors in therapeutics (Fan et al., 2018, Lis et al., 2018).

Due to the relative ease of measuring P-T73-Rab10 with this antibody, and its considered importance as a down-stream target of LRRK2, further experiments by the Alessi lab have considered the effects of other LRRK2 interactions with further proteins in the same signalling pathways, on Rab10. VPS35, a regulator of vesicles in intracellular trafficking (Progida and Bakke, 2016), and Rab29 are key upstream regulators of LRRK2. *Rab29* is one of five genes located at genetic locus PARK16, and an interaction between LRRK2 and this locus has been previously linked to PD. Meanwhile, overexpression of Rab29 has been found to rescue the shortened neurites phenotype found when pathogenic LRRK2 mutations and truncated Rab29 protein were expressed together (MacLeod et al., 2013). Rab29 regulates LRRK2 by interacting with its ankyrin domain. Subsequently phosphorylation of a key LRRK2 biomarker region between the ankyrin and kinase domains occurs, and LRRK2 localises to the Golgi apparatus or lysosome (Purlyte et al., 2018). Purlyte et al suggest that this mechanism could be duplicated with other Rabs at other membrane locations in order to activate LRRK2 around the cell. Rab29 is certainly not the only activator of LRRK2, as LRRK2 phosphorylated Rab10 even in Rab29-KO cells.

VPS35, which forms a complex with other proteins capable of activating LRRK2 (Figure 5), was first identified in several affected families (Vilarino-Guell et al., 2011). VPS35-D620N, a gain-of-function mutation, has been shown to up-regulate LRRK2-mediated phosphorylation of Rab10 in mouse lung, kidney, brain and spleen 6-fold, more than any known mutations in LRRK2 itself. PD patients with this SNP suffered corresponding phenotypes, with lower average age of onset (Mir et al., 2018). VPS35 is also located at the Golgi apparatus, and it is interesting that recruitment of LRRK2 to the Golgi results in loss of Golgi integrity, which could also be related to PD, although the mechanism by which this takes place is unknown (Purlyte et al., 2018).

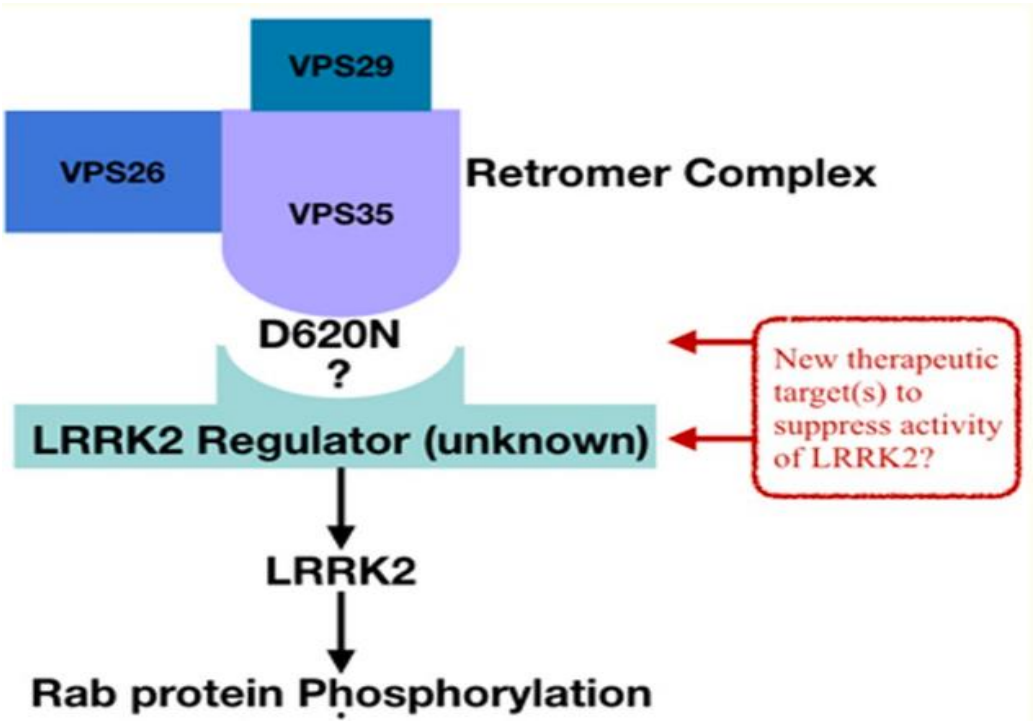

Figure 5. A putative pathway for LRRK2 (Mir et al., 2018). Up-regulation or overexpression of any protein component of this pathway may lead to Parkinson's disease, and all may be therapeutic targets.

1.3.4 Rab10 as a possible mechanism for LRRK2 pathology

Of the cohort of Rabs identified as LRRK2 substrates, Rab10 appears to have a much larger range of cell localisations and functions than most other Rab proteins, and thus over-phosphorylation of Rab10 is thought one of the most likely pathways to be a contributing factor to the development of PD. Increased expression of phosphorylated Rab10 has also been found in dopaminergic neurons of PD patients (Di Maio et al., 2018). Furthermore, roles for Rab10 have been identified in several processes which may influence the degeneration of dopaminergic neurons.

One of the most characterized roles of Rab10 is in mediating translocation of GLUT4 vesicles to the cell membrane, particularly in adipocytes. GLUT4 storage vesicles (GSVs) respond to insulin signalling by moving to and fusing with the plasma membrane, enabling expression of the GLUT4 glucose transporters on the cell surface for uptake of glucose to the muscles and adipose cells (Jaldin-Fincati et al., 2017). Rab10 is present in the membranes of GSVs in adipocytes (Larance et al., 2005). Insulin binding to the insulin receptor activates the PI3K pathway, resulting in the activation of Atk, which in turn phosphorylates AS160, a Rab-GTPase activating protein. AS160 switches on Rab10 by catalysing GDP-GTP exchange, and active Rab10 enables GSV translocation and docking. The mechanism for this is partially unknown, but it is likely that Rab10 recruits Myosin-Va, a molecular motor (Yoshizaki et al., 2007, Chen et al., 2012). With hyperactive LRRK2 causing the breakdown of the Rab10 cytosol-membrane recycling equilibrium, one effect would be to inhibit movement and fusion of GSVs, and limit the expression of GLUT4 transporters on the cell surface.

Phosphorylation of Rab10 by LRRK2 occurs as a response to lysosomal stress. Rab29 recruits LRRK2 to the overly full lysosomes, and LRRK2 is activated by the phosphorylation of the region between its kinase and ankyrin domains. LRRK2 is then able to phosphorylate Rab10 and Rab8, maintaining them on the lysosomal membrane and preventing their recycling. The Rab proteins then recruit effector

proteins EHBP1 and EHBP1L1, which increase protein secretion out of the lysosomes, possibly by means of vesicle formation to transport some of the lysosomal contents away (Eguchi et al., 2018). EHBP1 may also be recruited by Rab10 to aid lipid droplet engulfment by the autophagic membrane; in this instance EHD2 is also recruited, and the three form a complex between the autophagosome and lipid droplet (Li et al., 2016).

Rab10 has also been shown to have a role in mitophagy, adversely affected by over-phosphorylation by LRRK2. Mitophagy is of critical importance to the health of the cell, as defective mitochondria may produce excess reactive oxygen species (ROS) and release proapoptotic factors. Mitochondrial membrane potential is a key indicator of healthy mitochondrial function, as the membrane potential cannot be used to drive ATP production once it has dropped below a certain threshold; therefore, mitochondria depolarised below this threshold are tagged for destruction by mitophagy (Twig and Shirihai, 2011). Rab10 is recruited to depolarised and ubiquitin-labelled mitochondria, where it inserts into the membrane using its post-translational prenylation modification. Subsequently Rab10 binds OPTN, one of five primary autophagy receptors which are recruited to the mitochondria membrane. This is one of several mechanisms by which OPTN accumulates on the surface of the mitochondria, in accordance with the high volume of OPTN which is necessary for mitophagy to take place (Weil et al., 2018). However, the significant increase of T73-Rab10 phosphorylation caused by gain-of-function LRRK2 mutants impairs Rab10-OPTN binding, and mitophagy is disrupted (Wauters et al., 2019). Thus, defective mitochondria are not undergoing mitophagy at a normal rate, if at all, and the cells are at higher risk of damage from ROS and of undergoing apoptosis due to the release of proapoptotic factors. Oxidative stress, of which ROS are a principle cause, may also disrupt the binding of LRRK2 to activity-limiting 14-3-3 proteins and increase LRRK2 kinase activity even further (Lavalley et al., 2016, Di Maio et al., 2018). Mitochondria dysfunction has been reported in LRRK2 mutant cells, and was shown to be rescued by overexpression of Rab10, or by LRRK2 inhibition

(Wauters et al., 2019). It is notable that ROS-induced increase of LRRK2 kinase function would provide a mechanism by which LRRK2 activity may be responsible for aspects of PD development in more sufferers than just those with a LRRK2 gain-of-function mutation, giving greater potential impact to therapeutics which may be developed with LRRK2 and its substrates as targets.

Rab8A and Rab10 have also been identified as playing an important role in growth and development of cell cilia. It has been suggested that the role of Rab10 in ciliogenesis is as a suppressor. While Rab8A acts to give guidance for the positioning of apical markers, allowing ciliogenesis to begin (Sato et al., 2014), Rab10 co-localises to the base of primary cilia with RILPL1, where they prevent the creation of further cilia and the extension of pre-existing cilia. This is likely to occur through the characterised RILPL1 function of regulating cilia membrane content, specifically removing signalling proteins from the membrane (Schaub and Stearns, 2013). Rab10 is also able to initiate this process without RILPL1, but the opposite is not true (Dhekne et al., 2018).

Dhekne et al (2018) hypothesise that phosphorylation of Rab10 increases its affinity for binding RILPL1, and thus when LRRK2 is overactive, more Rab10-RILPL1 complexes are formed and the number and growth of cilia are reduced. Overexpression of Rab10 in A549 cells was also shown to significantly reduce the number and growth of cilia. Furthermore, when Rab10 or RILPL1 were knocked down, no difference in the cilia was observed between cells expressing gain-of-function LRRK2 mutations, and those expressing wild-type LRRK2, confirming that the pathway through which LRRK2 influences ciliogenesis is Rab10-RILPL1. Neurons and some glial cells are ciliated, and cilia have a vital role in the hedgehog (Hh) pathway and other signalling. There may therefore be potential for structural or signalling disruption in the brain when cilia protein components of the lipid membrane are altered or dismantled. A closer review of Hh signalling particularly reveals that

glycoprotein sonic hedgehog (Shh)-expressing dopaminergic neurons have a survival advantage over those where this has been ablated, as it provides them with resistance to neurotoxins MPTP and 6-OHDA. The resistance is generated by cholinergic (ACh) neurons' response to Shh, as they release GDNF, a neurotrophic factor, which is taken back up by the dopaminergic neurons (Gonzalez-Reyes et al., 2012). ACh neurons lacking properly functioning cilia are unable to take up Shh, and do not secrete GDNF. Interestingly, if this were a contributing mechanism to PD, it would mean that hyperactive LRRK2 in the ACh neurons was a cause in dopaminergic neuron death, rather than LRRK2 activity in the dopaminergic neurons themselves.

1.4 Aims and Objectives

My project hypothesis is that mechanisms of Rab10, one of the 23 Rabs present in both humans and in *Drosophila*, are affected by the gain-of-function mutations in LRRK2 which contribute to the development of PD. Extensive research identifying Rab10 as a substrate of LRRK2 has been performed principally in cells. The aim of the project is to investigate this interaction in a model organism, to confirm the genuine interaction *in vivo*. *Drosophila melanogaster* has been deemed a suitable model system in which to carry out this work, as the genome tractability and binary expression systems available will allow for the expression of Rab10 and LRRK2 variants to be tightly controlled, and because Rab10-KO is embryonic lethal in mice. Experiments will be carried out to ascertain whether altering the interactions of LRRK2 and Rab10 can negatively impact the speed and degree of tremor with which the fly can extend its proboscis. My objectives are therefore to cross fly lines to create Rab10/LRRK2 mutants, combinations and controls, to record the proboscis extension responses of these fly lines, and to analyse the footage to identify differences between fly lines in speed and tremor. Control lines will contain an optogenetic background controlled by the LexA-LexAop system, and lines containing additional combinations of Rab10-KO, Rab10 knockdown in

dopaminergic neurons, Rab10 overexpression, and LRRK2-G2019S expressed in dopaminergic neurons will also be created and analysed.

Materials and methods

2.1 Molecular Biology

2.1.1 Materials

The TAE buffer required for gel electrophoresis was created from 40mM Tris base, 20mM acetic acid and 1mM EDTA. Tris, acetic acid, EDTA and agarose were purchased from Melford. SYBR safe and 1kb ladder were purchased from Invitrogen. Primers for UAS were a kind gift from Dr Ryan West; all others were designed using Primer3 (http://primer3.ut.ee/) and PrimerX (http://www.bioinformatics.org/primerx/cgi-bin/DNA_1.cgi) and purchased from Sigma Aldrich.

Table 1. Primers used for genotyping *Gr5a* and *ReaChR*

Gene	**Primers (5'-3')**	**PCR product (bp)**
Gr5a	FW: TCCTACACGATGGCTCCTTC REV: GGAGCGATAAAGAGTGCGTG	~1500
ReaChR	FW: ARGAATTTGATAGCCCGGCG REV: ATCTTCTTCTTCCGCCACCA	~800

PCRs were performed using Master Mix from Invitrogen and Phusion kits manufactured by Finnzymes and Thermo Fisher. 'Squishing Buffer' for single fly DNA extraction was made from 10mM Tris, 25mM NaCl, and 1mM EDTA with 200ug Proteinase K added fresh to the Squishing Buffer prior to DNA extraction.

Drosophila melanogaster fruit flies were raised on cornmeal-sugar-agar-yeast food as described recently (Cording et al., 2017).

2.1.2 PCR with Taq

Primers were designed for genotyping for Gr5aLexA and ReaChR (Table 1). PCR was performed according to Invitrogen guidelines, using the cycling conditions in Table 2.

Table 2. Protocol for PCR using Taq polymerase.		
STEP	**TEMP**	**TIME**
Initial Denaturation	95°C	5 minutes
	95°C	30 seconds
	53°C	40 seconds
30 Cycles	72°C	1 minute/kb
Final Extension	72°C	5 minutes
Hold	4°C	∞

2.1.3 PCR with Phusion

PCR was performed according to Thermo Fisher guidelines, using the cycling conditions in Table 3.

Table 3. Protocol for PCR using Phusion		
STEP	**TEMP**	**TIME**
Initial Denaturation	95°C	30 seconds
	95°C	10 seconds
	61°C	30 seconds
30 Cycles	72°C	15 seconds/kb
Final Extension	72°C	5 minutes
Hold	4°C	∞

2.1.4 Gel electrophoresis

0.7% agarose gels were run at 100V.

2.1.5 Single fly DNA extraction

A pipette tip filled with 50ul combined Squishing Buffer and Proteinase K was used to mash a single fly in a 2ml tube. The Squishing Buffer was then ejected, and mixed without vortexing. The tube was kept at 37°C for 30 minutes, then at 80°C for 2 minutes and subsequently stored frozen until use. 1-2ul was used for each PCR.

2.2 Fly husbandry

Flies were kept in a warm room of 25°C with 12 hour cycling between light and dark, and fed with a solution of 5.5% agar, 22% cornmeal, 20.5% yeast and 52% sucrose. Nipagin was dissolved in ethanol and added to the mixture to prevent fungal growth in fly vials.

2.3 Measuring the Proboscis extension response

2.3.1 Feeding with retinal

Male flies were anesthetised and collected the day of hatching and moved into another vial. 24ul of retinal in DMSO (40 mM) was diluted in 1 ml 100 mM sucrose giving a 1 mM solution of retinal in sucrose. 300ul of this solution was pipetted onto the surface of standard food. The sucrose was used to encourage the flies to feed.

To prevent the flies drowning in the retinal solution, the tube was kept diagonal whilst the flies were anesthetised. When the flies were fully recovered, the tube was wrapped in tinfoil and stored for 3 days in the warm room (25°C).

2.3.2 Video Measurement of Proboscis Extension Response

Flies were trapped in pipette tips with the head protruding and secured using nail varnish to minimise movement of the head and legs. To ensure the flies would be hungry, and therefore responsive to the activation of Gr5a receptors, they were isolated in darkness for 2 to 3 hours.

The flies were positioned in a rig with a camera recording the fly magnified by a microscope. 470 nm wavelength light was flashed at the flies 10 times at regular intervals over 96 ms. The resultant proboscis extension responses were recorded in black and white by a Grasshopper 3 (Point Grey) camera (Figure 6). The Point Grey 'Flycapture' software was used to acquire ~4 seconds of footage at 258 frames per second, resulting in exactly 1000 frames. The video files were converted to images using Fiji (2.0 variant of ImageJ). Two approaches were used to analyse the proboscis extension: one to measure the increase in area of the image of the fly as the proboscis was extended, the second to measure the distance between the centre of the eye and the tip of the proboscis.

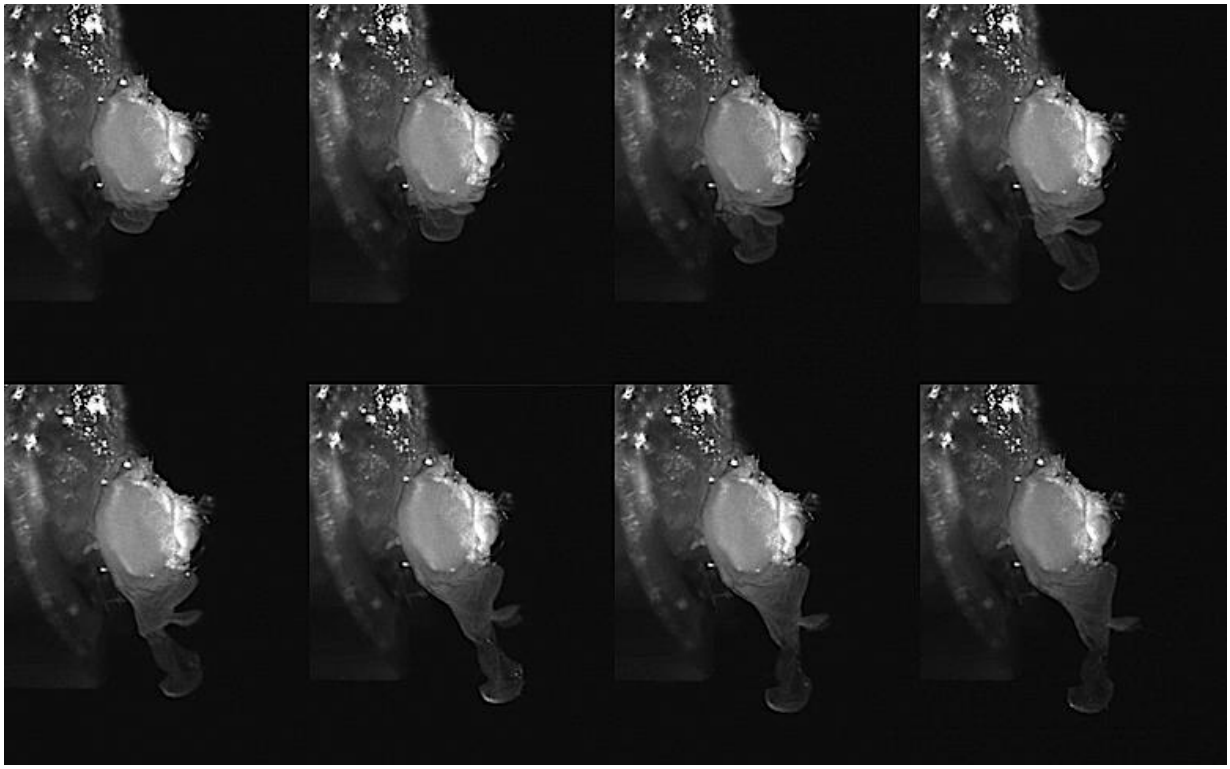

Figure 6. Series of frames from a recording of a *Gr5aLexA::LexAopReaChR* control fly proboscis extension response

2.3.3 Measurement of the proboscis extension

In order to find the movement of the proboscis, code (https://github.com/lcovill/fruit-flies-analysis-software/blob/master/core.clj) was run on 1000 images captured of each fly categorising each pixel as 'fly' (white) or 'background' (black) according to a darkness threshold which could be altered as necessary. The area of the white pixels was calculated for each image (Figure 7). The largest area of

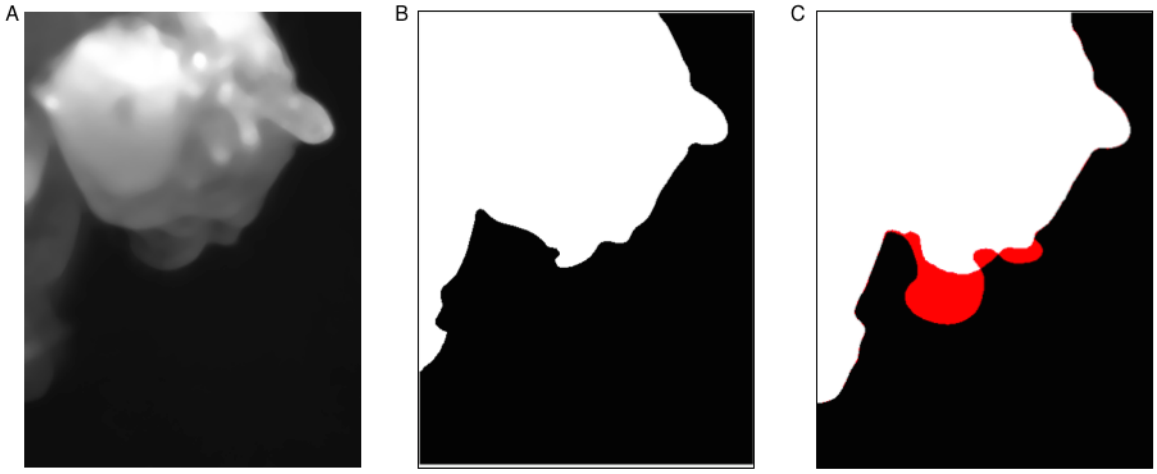

Figure 7. Post-analysis visuals of the calculated area of a fly head (A) An image of the fly head prior to light stimulation; (B) the same image after conversion to binary white 'fly' and black 'background'; (C) area in red of the extended proboscis.

'fly' before the area began to decrease again was taken as the end of initial extension, even if the area subsequently increased in later images as the fly re-extended its proboscis. The number of images from the beginning of the first flash to the initial maximum area was taken to be the duration of the initial extension, and the time between these frames in milliseconds was calculated for each fly. This approach is robust and straightforward and was used for Figure 11 and subsequently by Petridi et al [2019]. However, it did not provide a good estimate of tremor, because the variability in the pixel intensity around the edge of the fly head generated excess, false noise in measurement between frames. Thus, it was decided to measure tremor using a second approach.

2.3.4 Measurement of tremor in the Proboscis Extension Response

To calculate the degree of tremor present in the proboscis during the extension, code was written to select the lowest white pixel, with the portion of the image taken up by the pipette tip and any exposed leg excluded. Thus the lowest edge of the proboscis could be followed, and coordinates were generated. The coordinates of the proboscis tip for each fly were deposited into an excel file for analysis. Subsequently, coordinates over a threshold of x=400 which were generated when flashes occurred were removed.

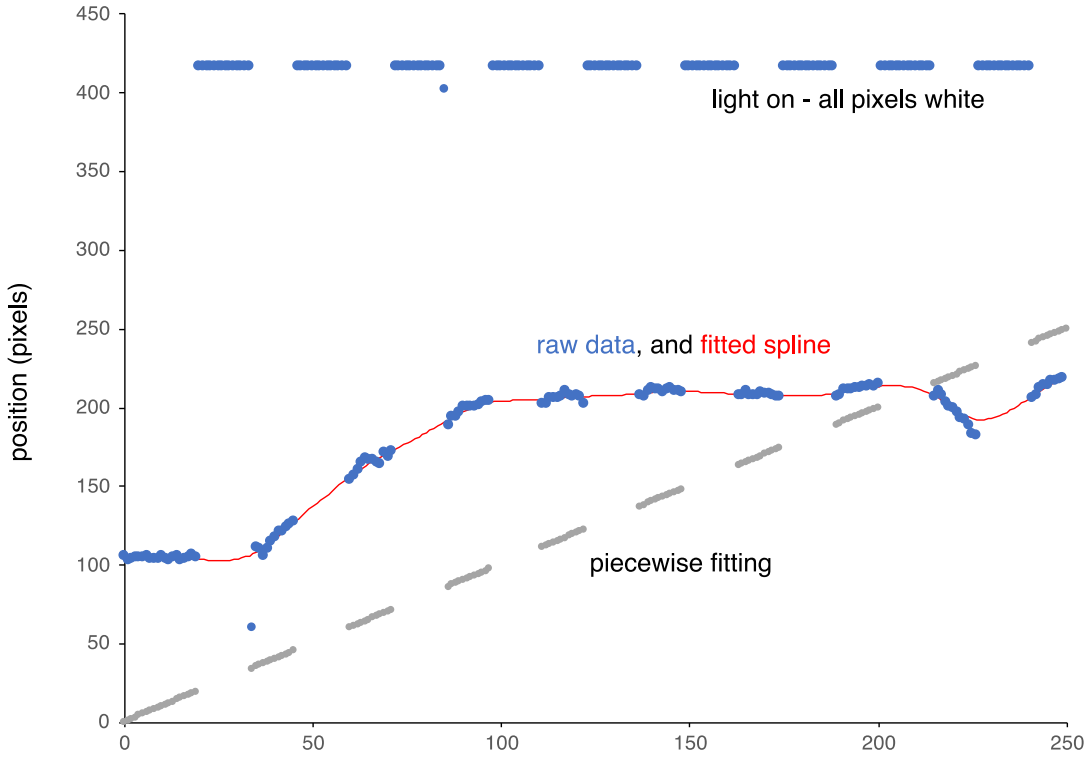

Figure 8. The Proboscis Extension Response is estimated from the piecewise cubic spline, estimated during each light-off period.

A second, median, filter removed single anomalous outlying coordinates. A problem arose as the response usually started before the 10 flashes were complete. In these second and subsequent flashes, the whole frame was 'white' and the area occupied by the fly was impossible to determine.

To fill in the position when the flash occurred, a continuous piecewise cubic spline was fitted to the data (Figure 8, http://zone.ni.com/reference/en-XX/help/371361P-01/gmath/cubic_spline_fit/). This approach was used for the data in Figures 10 and 13.

2.4 *Drosophila melanogaster*

2.4.1 Fly stocks

Table 4. Fly stocks

Table 4. Fly stocks; balanced stocks were obtained using routine fly genetics and provided as required. Crosses are indicated by / and recombined lines by ::		
Fly stock	**Abbreviation**	**Source**
Initial stocks		
TH-GAL4	*TH*	Kind gift of Serge Birman (Friggi-Grelin et al., 2003)
w^{1118}	*w-*	Elliott/Sweeney lab stock
Gr5aLexA	*Gr5aLexA*	Kind gift of Kristin Scott (Gordon and Scott, 2009)
w[*]; P{y[+t7.7] w[+mC]=lexAop-ReaChR} su(Chen et al.)attP5/CyO	*LexAopReachR*	Bloomington stock 53747
Rab10-	*Rab10 KO*	Kind gift of Robin Heisinger (unpubl). Deleted region is shown in Figure 12.
y[1] w[*]; P{w[+mC]=UASp-YFP.Rab10}13	*UAS-Rab10*	Bloomington stock 24097
y[1] v[1]; P{y[+t7.7] v[+t1.8]=TRiP.JF02058}attP2	*Rab10 RNAi*	Bloomington stock 26289 (used with UAS-Dicer2, Bloomington 24650)
UAS-G2019S	*G2019S*	Kind gift of Wanli Smith (Liu et al., 2008)
Recombined stocks		
TH::G2109S	*THG2*	*TH* and *G2019S* on 3rd

		chromosome
Gr5aLexA::LexAopReaChR	*Gr5a::OpR*	*Gr5LexA* and *LexAopReaChR* on second chromosome

2.4.2 Fly crosses

$$\frac{Gr5aLexA}{CyO} \times \frac{LexAopReaChR}{CyO}$$

$$\downarrow$$

$$\frac{Gr5aLexA}{LexAopReaChR} \ (Line\ 1)$$

♂ x ♀$\frac{Gr5aLexA::LexAopReaChR}{CyO}$

$$\downarrow$$

$$Gr5aLexA :: LexAopReaChR \ (Line\ 2)$$

$$w^{1118} \times \frac{Gr5aLexA :: LexAopReaChR}{CyO}; \frac{TH :: G2019S}{TM6B}$$

$$\downarrow$$

$$w^{1118}; Gr5aLexA :: LexAopReaChR; TH :: G2019S \ (Line\ 3)$$

$$\frac{Rab10KO}{FM7} \times \frac{Gr5aLexA :: LexAopReaChR}{CyO}; \frac{TH :: G2019S}{TM6B}$$

$$\downarrow$$

$$Rab10KO; Gr5aLexA :: LexAopReaChR; TH :: G2019S \ (Line\ 4)$$

$$UASRab10 \times \frac{Gr5aLexA :: LexAopReaChR}{CyO}; \frac{TH :: G2019S}{TM6B}$$

$$\downarrow$$

$$UASRab10; Gr5aLexA :: LexAopReaChR; TH :: G2019S \ \ (Line\ 5)$$

$$Rab10KO \times \frac{Gr5aLexA :: LexAopReaChR}{CyO}$$

$$\downarrow$$

$$Rab10KO; Gr5aLexA :: LexAopReaChR \ \ (Line\ 6)$$

$$\frac{Dicer2}{CyO}; \frac{Rab10^{RNAi}}{TM6B} \times \frac{Gr5aLexA :: LexAopReaChR}{CyO}; \frac{TH :: G2019S}{TM6B}$$

$$\downarrow$$

$$\frac{Gr5aLexA :: LexAopReaChR}{Dicer2}; \frac{Rab10^{RNAi}}{TH :: G2019S} \quad (Line\ 7)$$

$$\frac{Dicer2}{CyO}; \frac{Rab10^{RNAi}}{TM6B} \times \frac{Gr5aLexA :: LexAopReaChR}{CyO}$$

$$\downarrow$$

$$\frac{Dicer2}{Gr5aLexA :: LexAopReaChR}; Rab10^{RNAi} \quad (Line\ 8)$$

Results

3.1 Reliable optogenetic stimulation of the Proboscis Extension Response

3.1.1 A *Gr5aLexA*::*LexAopReachR* recombination

Previously flashes of blue light had been used to elicit the Proboscis Extension Response using crosses between the driver *Gr5aLexA* and responder *LexAopReaChR*. To facilitate further genetic manipulations, a potential recombinant stock *Gr5aLexA*::*LexAopReaChR*/CyO was provided. DNA was extracted from these flies and PCR primers for *Gr5aLexA* and *LexAopReaChR* were designed. Gel electrophoresis (Figure 9) confirmed that all flies contained both transgenes, while w^- controls had no bands.

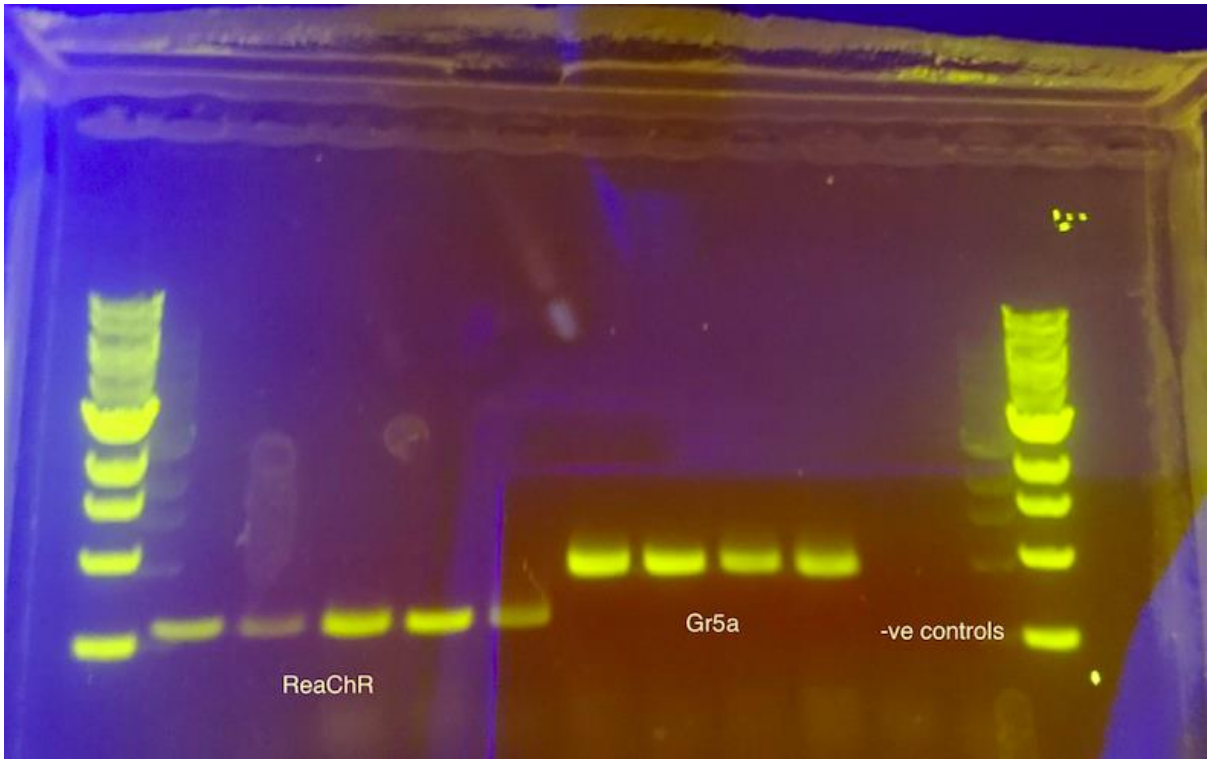

Figure 9. Gel electrophoresis of genotyping for *Gr5aLexA* and *ReaChR*. To ensure successful recombination of *Gr5aLexA* and *LexAopReaChR* had taken place, single fly DNA extraction was performed on flies thought to have the genotype *Gr5aLexA::LexAopReaChR*, and w^- control flies. Genotyping for *ReaChR* (600bp) and *Gr5aLexA* (1500bp) was performed on the extracted DNA using Phusion and the primers in Table 1. Lane 1, 1kb ladder. Lanes 2-6, PCR products of 5 *Gr5aLexA::LexAopReaChR* line flies genotyped for *ReaChR.* Lanes 7-10, PCR products of 4 *Gr5aLexA::LexAopReaChR* line flies genotyped for *Gr5aLexA.* Lane 11, PCR products of w^- fly genotyped for *ReaChR.* Lane 12, PCR products of w^- fly genotyped for *Gr5aLexA*. Lane 13, 1kb ladder.

To confirm this biologically, *Gr5aLexA*::*LexAopReaChR* homozygotes were selected and fed retinal for 3 days. Their Proboscis Extension Response in response to a flash of blue light was recorded and compared with the *Gr5aLexA*/*LexAopReaChR* cross. Both lines successfully extended their proboscis, demonstrating effective recombination.

3.1.2 Typical proboscis extension response trace

A typical recording is shown at https://www.youtube.com/watch?v=Zy4qGGrn1ro . In this a series of 10 flashes is used to stimulate the *Gr5aLexA::LexAopReaChR* fly, and it extends its proboscis. For each dark frame, the area of the fly is measured, and the area increases as the proboscis is extended. However, in each flash, the outline of the fly is lost, as during that time the entire frame appears white. Distortion may occur due to a pixel elsewhere in the shot being illuminated in a single frame. The sample trace shows two examples of this (at ~30 and ~260 frames). Many flies retract the proboscis after initial extension (see frames 200-300 of the sample trace) and may or may not re-extend, while others maintain extension due to subsequent flashes preventing repolarisation of the Gr5a neurons.

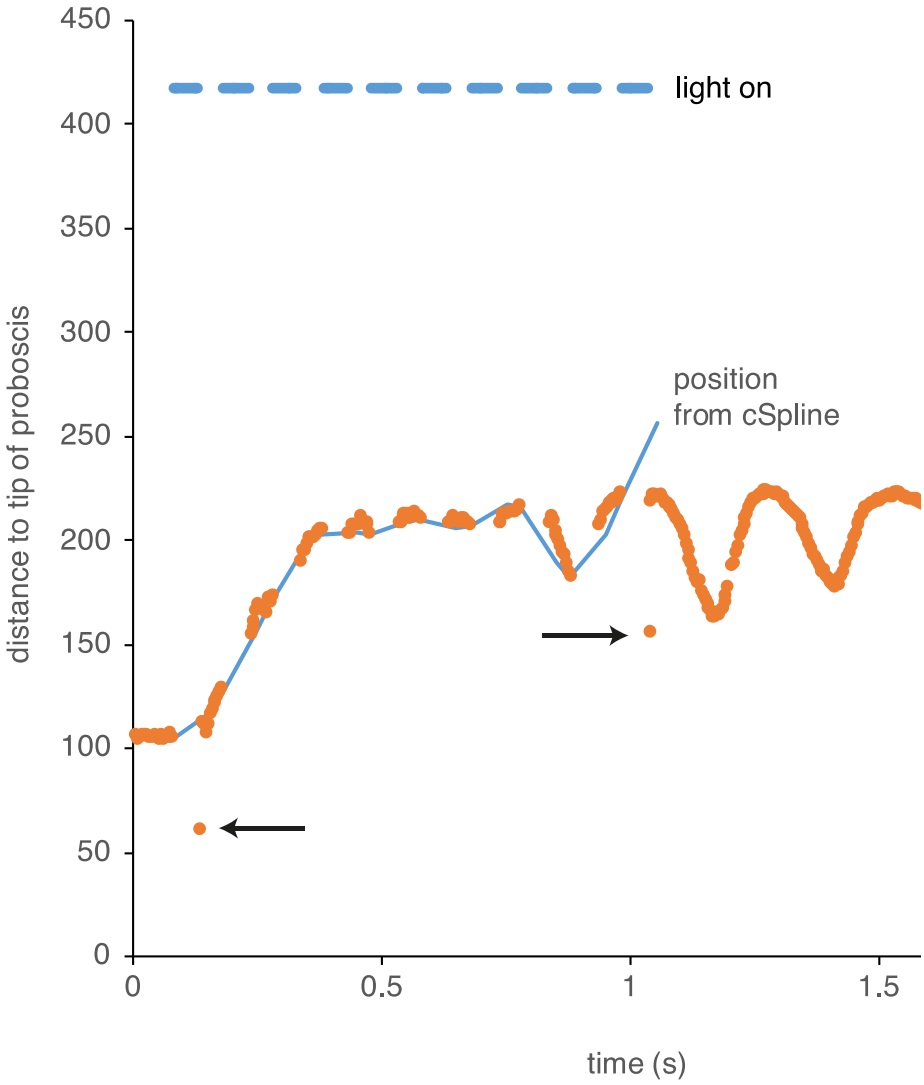

Figure 10. Trace of the tracked proboscis (orange) which is lost during flashes (blue) with fitted continuous piecewise cubic spline. Proboscis extension occurs after ~60 ms, and is complete by 400 ms. Note the two deviant points (black arrows), and the fit between the cubic spline and the observed data. After ~1 s, further movements occur. Fly genotype *Gr5aLexA/LexAopReaChR*.

3.1.3 Analysis of control lines containing *Gr5aLexA* and *LexAopReaChR*

Two control lines were tested: the *Gr5aLexA/LexAopReaChR* cross and the *Gr5aLexA::LexAopReaChR* homozygotes. The mean time for the control flies to completely extend the proboscis after the initial flash trigger was consistent, with means of the control lines being 393.4 ± 40.3 ms

(*Gr5aLexA*/*LexAopReaChR*) and 412.3 ± 26.0 ms (*Gr5aLexA*::*LexAopReaChR*) (Figure 11A). In an ANOVA, the post-hoc Dunnett's T-test showed no significant difference between these lines. Although there is a slight difference in latency between these two control genotypes, this is similar to the difference in time to fully extend, which was not significant.

In addition, a third line was used in which two UAS constructs were present, but no GAL4: *Gr5aLexA::LexAopReaChR/Dicer2; Rab10 RNAi.* In this control, the time to peak extension of the proboscis was 311 ± 23 ms, not significantly faster than the outcross flies with only *Gr5aLexA/LexAopReaChR* (Figure 11). The latency was 57 ± 24 ms, making the response quite variable, and not significantly different from the control outcross.

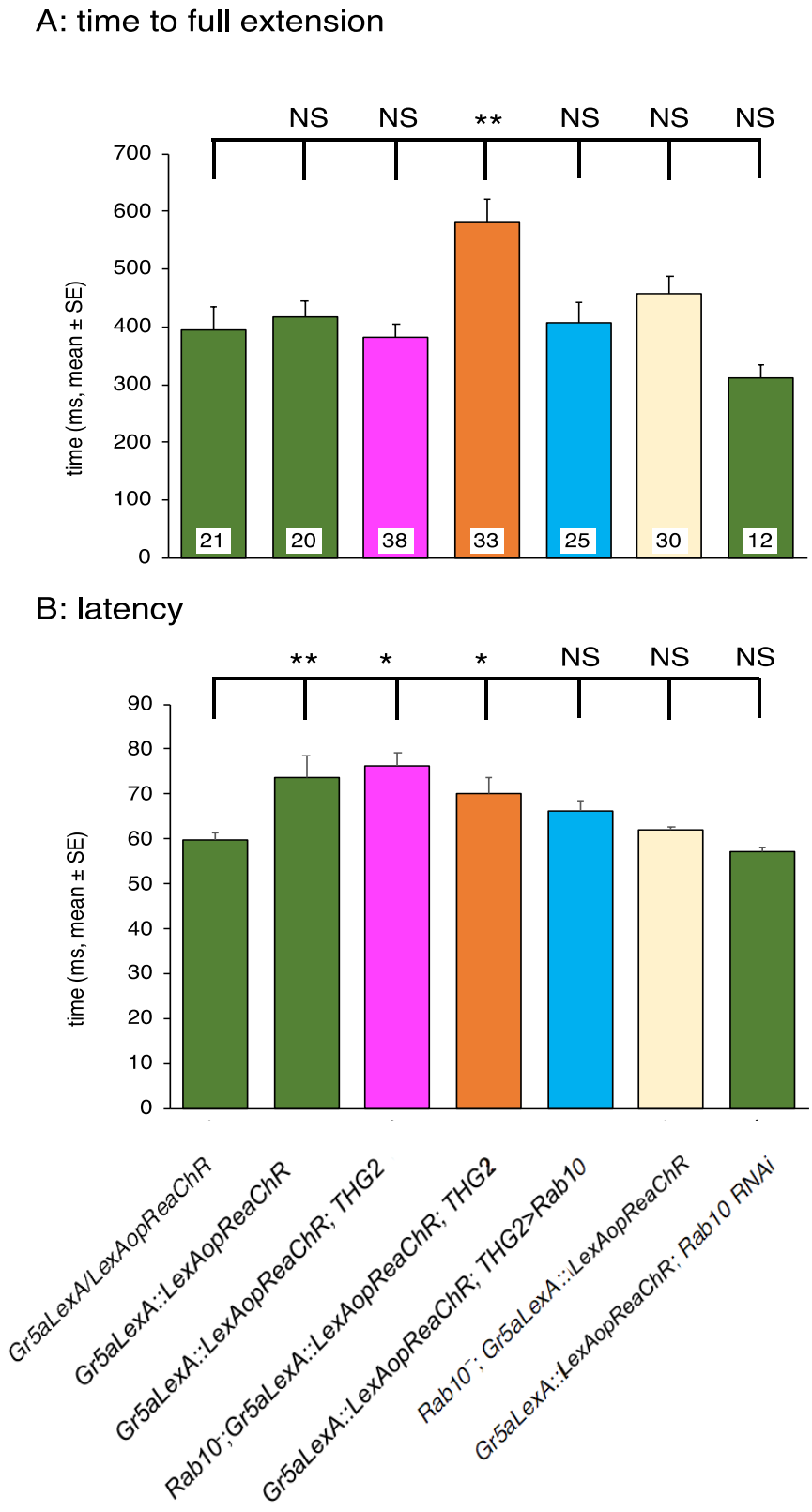

Figure 11. Flies with both *Rab10*$^{-}$ and *TH>G2019S* are much slower to extend the proboscis than any other genotype. A. Time to reach maximum extension. B. Time to start extending the proboscis. Although there are statistically significant differences in the latency, these are small compared with the effect of *Rab10*$^{-}$ and *TH>G2019S* on the time to fully extend.

3.2 Interaction of Rab10 and LRRK2 *in vivo*

It was suggested by Steger et al (Steger et al., 2016, Steger et al., 2017) that LRRK2 phosphorylated Rab10 and that this was the main action of LRRK2 *in vitro*. The main purpose of this report is to examine this *in vivo* in the fly model of Proboscis Extension.

3.2.1 Alignment of human and *Drosophila* Rab10

First, a bioinformatics approach was taken to see if it was likely that human LRRK2 might phosphorylate fly Rab10. It was necessary to discover whether the sequence of Rab10 conserved, particularly at the putative phosphorylation site.

An alignment was created demonstrating the conservation of Rab10 protein between the human and *Drosophila* systems (Figure 12). The conserved P-loop and Switch 1 and 2 regions were found in the amino acid sequences of human and *Drosophila* Rab10 by using identifiers listed in Coppola et al., [2016]. dRab10 and hRab10 are identical in the Switch 2 and P-loop regions, with 1 amino-acid difference at the start of Switch 1. However, much of the tail region is not conserved (amino-acids 170-200) so that the total hRab10 antibody which is targeted at this region is unlikely to recognise dRab10. The last four amino-acids – where prenylation occurs – are also identical. Notably, the binding site for the phospho-Rab10 antibody (amino-acids 67-80) also has the same sequence. This is the site at which LRRK2 will bind and phosphorylate Threonine 73. All of this suggests that it would be feasible for human LRRK2 to phosphorylate dRab10 at an equal rate as it phosphorylates hRab10. dRab10 is found in many neurons (Zhang et al., 2007), so that neuronal expression of LRRK2 could increase the amount of P-73-Rab10, and this was subsequently demonstrated (Petridi et al, 2019).

A fly Rab10^{-} null was provided, in which the amino acids 21-end were deleted. This deletes the entirety of switch 1 and 2, the P-loop, and the tail, so that there is no possibility of LRRK2 interacting with any residual protein. No P-73-Rab10 was detected in the Rab10^{-} null fly (Petridi et al, 2019).

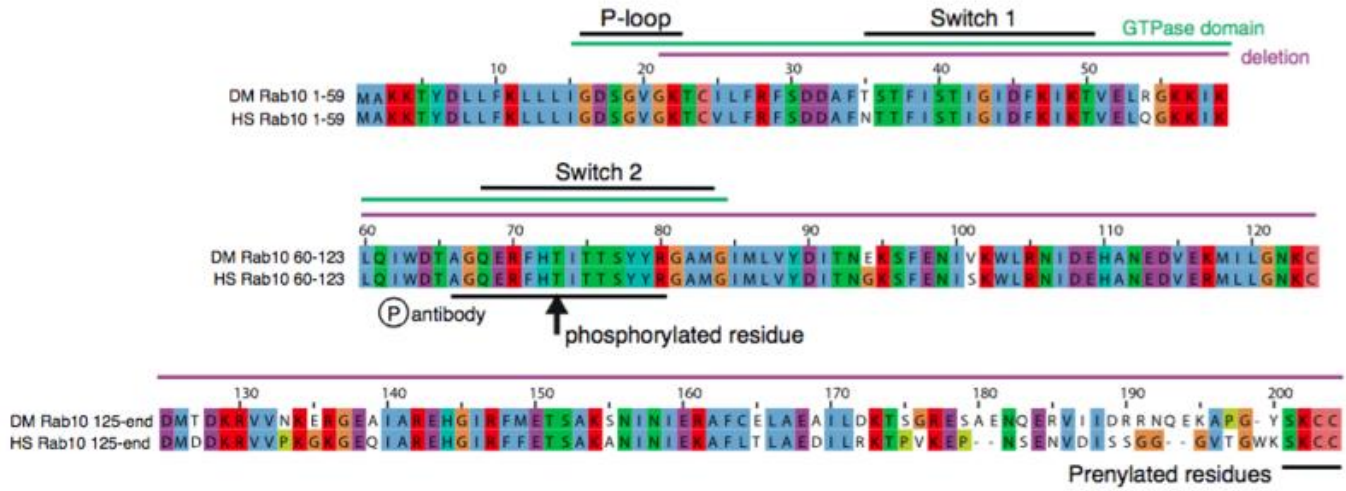

Figure 12. Alignment of human and *Drosophila* Rab10 protein sequences. The GTPase domain is highlighted in green; the P-loop, Switch 1 and Switch 2 regions in black (Coppola et al., 2016); and the deletion in the Rab10 knockout flies in purple. The binding site for the Rab10 antibody, the threonine residue which is phosphorylated by LRRK2, and the two cysteine residues which are prenylated by Rab geranylgeranyltransferase are also labelled**.** Sequences were procured from UniProt (hRab10 accession no. P61026; dRab10 accession no. O15971) and the alignment was created using JalView and edited and labelled in Adobe Illustrator.

3.2.2 Flies with both *Rab10*$^{-}$ and dopaminergic expression of *LRRK2-G2019S* have a slower Proboscis Extension Response.

For comparison with the sucrose response of flies expressing *LRRK2* transgenes in their dopaminergic neurons, the *TH::G2019S* recombinant was introduced into the optogenetic background, *Gr5aLexA::LexAopReaChR.* When stimulated with blue light, the time to reach the peak extension was 381 $\pm$ 22 ms (Figure 11), which is not significantly different from the Line 1 control *Gr5aLexA/LexAopReaChR.* Similarly, with *Rab10*$^{-}$ null in the same optogenetic background, the mean time to extend the proboscis was 461 $\pm$ 31 ms, again not significantly different from the Line 1 control (Figure 11).

However, when both *Rab10*$^{-}$ and *TH::G2019S* transgenes were deployed, the Proboscis Extension Response took much longer, 579 $\pm$ 41 ms, (Dunnett post hoc test, P = 0.0044) (Figure 10). This represents a 50% increase in extension time. In this situation Rab10 is eliminated globally, while *G2019S* is expressed in dopaminergic neurons.

This poses the question of whether it is the Rab10 <--> LRRK2 interaction is dopaminergic neurons that is key, or whether LRRK2 has an effect in the dopaminergic neuron, while Rab10 acts in another neuron subset or in the muscle. To address this, *Rab10* was knocked down using RNAi in the dopaminergic neurons. The effectiveness of this RNAi line is shown in western blot for P-T73-Rab10 (Petridi et al 2019).

The original cross to generate dopamine specific *Rab10* RNAi and *G2019S*, produced few male offspring of the desired genotype Gr5aLexA::LexAopReaChR/Dicer2; Rab10^{RNAi}/TH::G2019S, leading to the cross being repeated. The second cross produced more offspring, however all but 2 of these died before or during preparation for Proboscis Extension Response, specifically during the 2-3 hour incubation whilst trapped in pipette tips. Although proboscis extension responses were achieved with these 2 surviving flies, analysis was not performed on the results due to lack of power. The flies may not have been able to withstand the 2 hour starvation, due perhaps to too much DMSO (which can result in flies eating less), and flies may drown in the solution if they are not completely recovered from being anesthetized when the vial is returned to a vertical position. It is noted that the dopaminergic expression of *Rab10* RNAi and *LRRK2-G2019S* was subsequently shown to result in a slower Proboscis Extension Response (Petridi et al, 2019).

Finally, the hypothesis that increased dopaminergic *Rab10* expression with *LRRK2-G2019S* might generate a phenotype was tested.

3.2.3 Effect of increased Rab10 expression

It was also important to test if additional dopaminergic expression of Rab10, with *LRRK2-G2019S*, affected the flies. UAS-Rab10 and *LRRK2-G2019S* were both driven by TH-Gal4 in the dopaminergic neurons, in the optogenetic background. In fact, while the mean extension time of 407.75 ± 34 ms was not significantly different from the times taken by the control lines, these flies had difficulty fully extending their proboscises, with most experiencing a truncated response. This line also experienced spontaneous tremor during and after the PER was triggered (https://www.youtube.com/watch?v=_0cHnyNpRTg – the tremor and extension can be clearly seen at 0.25 speed).

3.2.4 Latency to beginning of the Proboscis Extension Response

The difference in latency to the start of the PER is statistically significant ($F_{1,6.629} = 6$, $P < 0.005$) (Figure 10). However, this difference may be due difficulties in determining the exact start of the movement, as flies of the same line display variation of ~13 ms. Furthermore, the control lines 1 and 2, which contain no transgenes or mutations, contain the shortest latency (*Gr5aLexA/LexAopReaChR*, mean=59.69±1.697), and one of the longest latencies (*Gr5aLexA::LexAopReaChR*, mean=73.828±4.758). This highlights the difficulty of assessing the start of the PER movement, which may be partly obscured by the second light flash. Indeed, in some cases, it is clear that the Proboscis Extension Response only began after the second or third flash (Figure 13A).

3.3 Summary of the effect of LRRK2 and Rab10 variants on the speed of PER

Thus, overall, the data supports the idea that Rab10 and LRRK2 interact in dopaminergic neurons. Only the combination of both manipulations in the same neuron was effective in prolonging the Proboscis Extension Response.

3.4 Tremor of proboscis extension response

The analysis of the movement of the proboscis allows for the estimation of latency and time to full extension. However, in the sucrose stimulated data collected by Cording et al [2017] it was shown that the expression of *G2019S* or *I2020T* in dopaminergic neurons increased the amount of tremor. Tremor was measured as the difference between the actual data and the cubic spline fit (Figure 13B). For each trace, the data and cubic spline was calculated, and the absolute value of the difference was determined. The median of these absolute differences was calculated for each fly.

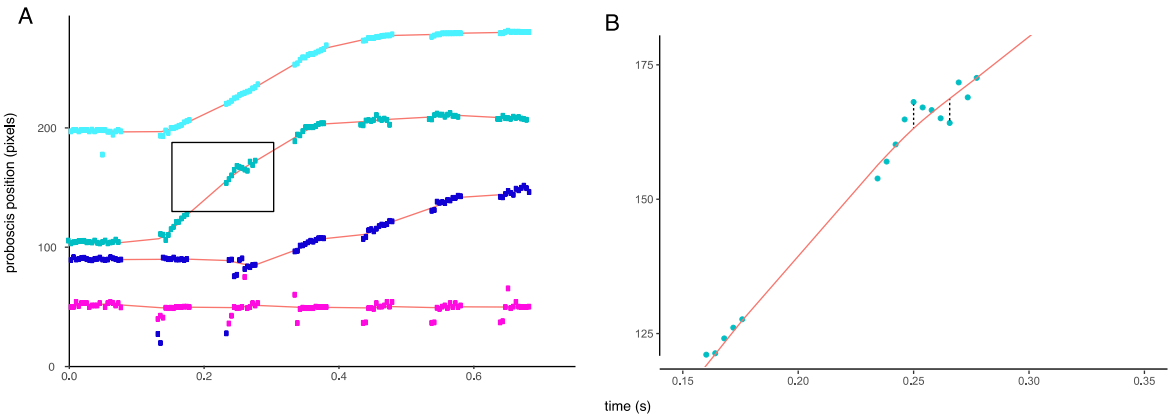

Figure 13. Analysis of the Proboscis Extension Response for tremor. Observed data as points, fitted cubic spline as red line. A. Four sample traces. The top and second traces (cyan and green) show a short latency response. The third trace (dark blue) shows a much longer latency. The lowest trace shows that the analysis fails to measure any extension of the proboscis. B. Measurement of the absolute deviation between spline (red line) and data, as indicated by the dotted black lines. The data corresponds with the box in A.

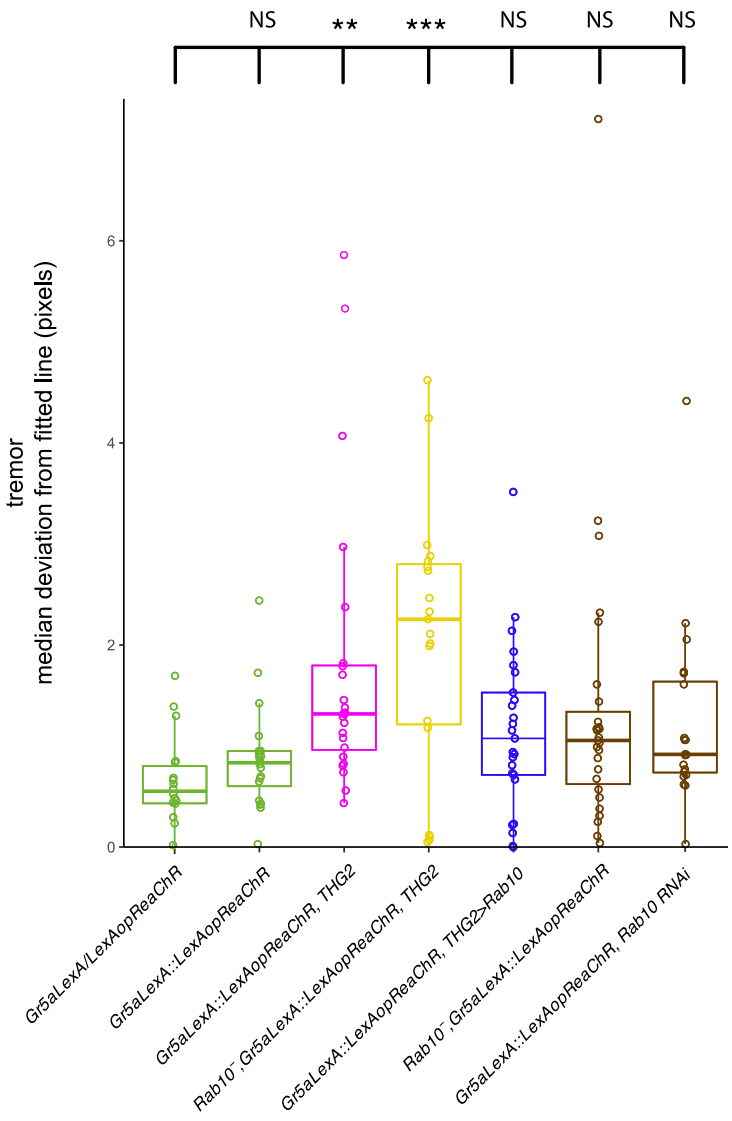

Figure 14. Dopaminergic expression of *LRRK2-G2019S* (magenta) increases tremor and this is not blocked by the *Rab10*¯knock-out (yellow). Controls are green, Rab10 overexpression blue, and Rab10 reduction in brown. There is no significant difference between the flies expressing *LRRK2-G2019S* with and without Rab10 (*Gr5aLexA*::*LexAOpReachR;THG2* against *Rab10*¯;*Gr5aLexA*::*LexAOpReachR; THG2).*

Overall, this shows that the tremor is substantially increased when *G2019S* is expressed in dopaminergic neurons. The control flies (*Gr5aLexA/LexAopReaChR* green bar) have average tremor (0.87 ± 0.11) but the dopaminergic *G2019S* flies have about twice as much (1.78 ± 0.29, magenta). This is not affected in the *Rab10*¯ background (mean 2.05 ± 0.30, yellow bar). As with other fly

phenotypes *TH>G2019S* flies show a very variable penetrance, with large SE irrespective of the presence of Rab10. In the control background, increasing Rab10 (blue) or reducing it (brown) has no effect.

Discussion

The key results are that the Proboscis Extension Response (PER) can be elicited consistently by optogenetic stimulation, that the speed of extension is reduced only in the double transgenic, Rab10^{-} and *TH>G2019S*, while just *TH>G2019S* is enough to induce tremor. The setup also allows us to test the accuracy of image digitisation and automated computer analysis of proboscis extension.

4.1 Differences in the PER of *TH > G2019S* flies between optogenetic and sucrose stimulation

Flies responded reliably to the 10 flashes of blue light, with the PER usually beginning shortly after the first flash. In the control lines, almost all the flies responded to the light with a PER, demonstrating the efficacy of this method of achieving a PER and reliability of the response once a protocol was well-established for these flies. Furthermore, there was no evidence that more *TH>G2019S* flies failed to respond than control flies. This data contrasts with that of Petridi et al (2019) where a single flash of light was used as the stimulus. They used the same transgenic constructs and apparatus, but found that *TH>G2019S* flies had a less frequent, slower response – i.e. showed both bradykinesia and akinesia. The difference between the data here (where *TH>G2019S* had the same speed of response as controls) and the slower extension described by Petridi et al (2019) may be due to the fact that they kept the flies at 29°C for 7 days to increase expression. Equally, it appears that the multiple flashes of light used here generated more action potentials in the *Gr5a* neurons and provided a more reliable stimulus than the single flash of Petridi et al (2019).

In the response to sucrose, Cording et al (2017) also found that the *TH>G2019S* and *TH>I2020T* lines had a slower response than controls, whereas in this project, the mean time to maximum extension of the proboscis in *TH>G2019S* flies was not significantly different to the control flies. Cording et al kept flies at 29°C for 3 days after eclosion, increasing the expression of proteins driven by Gal4 as stated above. Furthermore, there was an experimental difference in presentation of the stimulus, which could lead to a difference in neuronal response. Cording et al (2017) only stimulated the legs with sucrose, whereas *Gr5a* expression occurs in sensory neurons in both proboscis and legs (Chyb et al., 2003). The proboscis neurons and leg neurons trigger different responses, with only activation of the leg neurons provoking a PER. Proboscis *Gr5a*-expressing neurons activate taste neurons after initial presentation of a food or substance, to signal for further food intake, or rejection. It is possible that the proboscis *Gr5a* and leg *Gr5a* were stimulated optogenetically, while the sugar solution used by Cording et al acted only on the legs; whether or not this is the case, it would occur across all the tested lines including controls.

The standard deviation of proboscis extension speed was high for all the fly lines, but the scatter of the data was most for the double transgenic, *Rab10*$^{-}$ and *TH>G2019S*. Similarly, when the *LRRK2-G2019S* allele is expressed in humans, it has extremely variable penetrance (Healy et al., 2008a). This indicates that as in humans, LRRK2 and Rab10 do not operate in isolation to cause Parkinsonian symptoms in Drosophila, but rather increase susceptibility of the flies to other genetic or environmental factors, which combine to cause the slowness and tremor observed in some of the flies.

Both the data presented here and that from Cording et al (2017) indicate that the *TH>G2019S* flies show tremor. In at least some of the flies recorded here, the tremor is seen at rest, with the double transgenic (*TH>G2019S*, *UAS-Rab10*) showing marked resting tremor. This automated recording of tremor, which is not affected by operator variability in sucrose presentation, provides the first unbiased measure of the Parkinson's disease related phenotype in flies.

4.2 Analysis of the effect on PER by Rab10 knock-out

The double transgenic *Rab10*$^{-}$ and *TH>G2019S,* shows a synthetic bradykinesia phenotype, as neither the *Rab10*$^{-}$ (Line 6) nor the *TH>G2019S* (Line 3) lines show this phenotype. The *Rab10*$^{-}$ is a global null, and the *TH>G2019S* is dopaminergic expression. In extending these observations, Petridi et al (2019) found that dopaminergic knock-down completely ameliorated the *TH>G2019S* proboscis extension phenotype. This shows a difference between the global and dopaminergic knock-down of Rab10.

The *in vitro* data generated by Alessi's group suggests that Rab10 is phosphorylated by LRRK2 (Steger et al., 2016). If this were to occur *in vivo*, the prediction was that flies with both knock-down of *Rab10* and dopaminergic expression of *G2019S* should have had slower extension and increased tremor caused by disrupted vesicular transport in dopaminergic neurons, as found by Petridi et al. [2019]. Specific activities of hyperphorphorylated Rab10, such as preventing normal expression of GLUT4 transporters to the cell surface, improperly dealing with lysosomal stress, and preventing defective mitochondria from efficiently beginning mitophagy, may equally play a role in the development of this phenotype. Further experiments could be performed to establish these in the cell, for instance by measuring intracellular ROS levels by fluorometric determination.

The synthetic interaction between *TH>G2019S* and *Rab10*$^{-}$ is different from this, and suggests that the Rab10 is having an effect elsewhere in the proboscis extension neural circuit. The main parts of the circuit are the Gr5a sensory neurons, the motor neurons and muscles. The genetic tools are available to achieve *Rab10* knock-down in these components: e.g. *Gr5a-GAL4*, *OK-6-GAL4* and *mhc-GAL4* respectively. Further it would be constructive to compare the effect of *Rab10*$^{-}$ with a global knock-down of *Rab10* using a ubiquitous *GAL4* (for example, *Actin5c* or *daughterless*).

It is possible that the *Rab10*$^{-}$ has a second, off-target, mutation, which could explain the synthetic bradykinesia. To test this, it would be good to examine flies carrying both the *Rab10*$^{-}$ and expressing

UAS-Rab10:

$$Rab10KO\ ;\ \frac{Gr5aLexA :: LexAopReaChR}{UAS - Rab10}\ ;TH - Gal4 :: G2019S$$

In such flies, Rab10 will be present in the dopaminergic neurons and would be expected to ameliorate any effects of the Rab10 null in these neurons.

The data collected by Petridi et al (2019) confirmed *in vivo* that Rab10 could be phosphorylated by LRRK2, using the phospho-Rab10 antibody. To test this further, rescue flies could be created in which *Rab10* is replaced by a form which could not be phosphorylated or prenylated:

$$Rab10KO\ ;\ \frac{Gr5aLexA :: LexAopReaChR}{UAS - Rab10 - modified}\ ;TH - Gal4 :: G2019S$$

5.3 Analysis of digitisation

Two automated methods to determine the proboscis extension were tried (1) measuring the area of the fly head and (2) measuring the distance from the tip of the eye to the end of the proboscis. Method 1 suffered from errors in creating the binary (black/white) image from the head of the fly, which gave very variable area estimates from frame to frame. Method 2 was much more accurate, with consistent distances. This allowed the estimation of tremor which varies by genotype. However, if the fly rotates the head, so that the proboscis is not extended in a direct line, the actual extension may be underestimated. An example of this is shown in Figure 13 (magenta line). A second problem noted was that some flies, particularly those with the *UAS-Rab10* construct, failed to fully extend their proboscis, which makes an automated system hard to achieve. Such partial extension may reflect a 'hypokinesia' phenotype, and it would be worth developing software further to measure this.

Both methods suffered from the fact that proboscis extension began before the last flash had been given. Using a single flash, over before the start of the response, allowed Petridi et al [2019] to use

similar code to determine a more accurate trajectory, although it also meant that more flies must be tested to achieve the same power in statistical tests, as fewer of the flies exposed to a single flash produced a PER.

Future Perspectives

There is great scope for further research of Rab10's role in Parkinson's Disease. In light of Rab10 being established as a likely next step in the pathway including VPS35, Rab29 and LRRK2, a new angle searching for PD therapies is to establish a mechanism whereby Rab10 over- or under-expression may disrupt rate of glucose uptake, lysosomal stress relief, and mitophagy. The interaction between LRRK2 and Rab10 may also be important in pathogen neutralisation (Herbst and Gutierrez, 2019). It remains to be seen how LRRK2 signals in Crohn's disease and in melanoma.

A role for Rab10 in Alzheimer's disease has been identified. A rare SNP in the 3'-untranslated region of Rab10 was found to confer significant resilience to individuals even with the major risk factor APOE ε4 allele, and knockout of Rab10 in vitro reduced the amount of a toxic variant of amyloid β (Aβ) protein found in cells (Tavana et al., 2019). Rab11 has been found to possibly function through amyloid clearance (Udayar et al., 2013). T-73-Rab10 has also been found to co-localise with Aβ plaques, and may contribute to Aβ build-up through reduced function of Rab10 allowing accumulation of Aβ in a similar mechanism to that of Rab11 (Yan et al., 2018). It is too early to tell if this is also linked to LRRK2 or if phosphorylation of Rab10 in Alzheimer's is due to other kinases.

However, the main impact of this work is on PD. Effects of LRRK2 and Rab10 on bradykinesia and tremor were determined in an unbiased, automated way in the fly model of PD. These effects occurred exclusively in dopaminergic neurons. In humans too, people with PD develop these phenotypes due to loss of dopaminergic neurons. As the condition advances, and progresses to akinesia or hypokinesia, they may be often incapacitated by severe tremor to the extent that

surgical intervention is considered preferable. It is logical therefore to maintain focus on activities of these proteins within dopaminergic neurons.

Abbreviations

ACh: Cholinergic neuron

CDR: Complementarity determining region

CNV: Copy number variant

DMSO: Dimethyl sulphoxide

EDTA: Ethylenediaminetetraacetic acid

GSV: Glucose storage vesicle

GWAS: Genome Wide Association Study

KD: Knock-down

KO: Knock-out

LC-MS: Liquid chromatography-mass spectrometry

L-Dopa: Levidopa

PCR: Polymerase chain reaction

PD: Parkinson's Disease

PER: Proboscis extension response

RNAi: RNA interference

ROS: Reactive oxygen species

SDS-PAGE: Sodium dodecyl sulfate–polyacrylamide

SNP: Single nucleotide polymorphism

TAE: Tris-acetate-EDTA

References

ARMSTRONG, R. A. 2008. Visual signs and symptoms of Parkinson's disease. *Clin Exp Optom,* 91**,** 129-38.

BAE, E. J., KIM, D. K., KIM, C., MANTE, M., ADAME, A., ROCKENSTEIN, E., ULUSOY, A., KLINKENBERG, M., JEONG, G. R., BAE, J. R., LEE, C., LEE, H. J., LEE, B. D., DI MONTE, D. A., MASLIAH, E. & LEE, S. J. 2018. LRRK2 kinase regulates alpha-synuclein propagation via RAB35 phosphorylation. *Nat Commun,* 9**,** 3465.

BAPTISTA, M. A., DAVE, K. D., FRASIER, M. A., SHERER, T. B., GREELEY, M., BECK, M. J., VARSHO, J. S., PARKER, G. A., MOORE, C., CHURCHILL, M. J., MESHUL, C. K. & FISKE, B. K. 2013. Loss of leucine-rich repeat kinase 2 (LRRK2) in rats leads to progressive abnormal phenotypes in peripheral organs. *PLoS One,* 8**,** e80705.

BARDEN, H. & LEVINE, S. 1983. Histochemical observations on rodent brain melanin. *Brain Res Bull,* 10**,** 847-51.

BEAL, M. F. 2010. Parkinson's disease: a model dilemma. *Nature,* 466**,** S8-10.

BENTO, C. F., PURI, C., MOREAU, K. & RUBINSZTEIN, D. C. 2013. The role of membrane-trafficking small GTPases in the regulation of autophagy. *J Cell Sci,* 126**,** 1059-69.

BRAND, A. H. & PERRIMON, N. 1993. Targeted gene expression as a means of altering cell fates and generating dominant phenotypes. *Development,* 118**,** 401-15.

BREDA, C., NUGENT, M. L., ESTRANERO, J. G., KYRIACOU, C. P., OUTEIRO, T. F., STEINERT, J. R. & GIORGINI, F. 2015. Rab11 modulates alpha-synuclein-mediated defects in synaptic transmission and behaviour. *Hum Mol Genet,* 24**,** 1077-91.

BURBULLA, L. F., SONG, P., MAZZULLI, J. R., ZAMPESE, E., WONG, Y. C., JEON, S., SANTOS, D. P., BLANZ, J., OBERMAIER, C. D., STROJNY, C., SAVAS, J. N., KISKINIS, E., ZHUANG, X., KRUGER, R., SURMEIER, D. J. & KRAINC, D. 2017. Dopamine oxidation mediates mitochondrial and lysosomal dysfunction in Parkinson's disease. *Science,* 357**,** 1255-1261.

CAUCHI, R. J. & VAN DEN HEUVEL, M. 2006. The fly as a model for neurodegenerative diseases: is it worth the jump? *Neurodegener Dis,* 3**,** 338-56.

CHAN, S. L. & TAN, E. K. 2017. Targeting LRRK2 in Parkinson's disease: an update on recent developments. *Expert Opin Ther Targets,* 21**,** 601-610.

CHEN, Y., WANG, Y., ZHANG, J., DENG, Y., JIANG, L., SONG, E., WU, X. S., HAMMER, J. A., XU, T. & LIPPINCOTT-SCHWARTZ, J. 2012. Rab10 and myosin-Va mediate insulin-stimulated GLUT4 storage vesicle translocation in adipocytes. *J Cell Biol,* 198**,** 545-60.

CHINTA, S. J. & ANDERSEN, J. K. 2005. Dopaminergic neurons. *Int J Biochem Cell Biol,* 37**,** 942-6.

CHUTNA, O., GONCALVES, S., VILLAR-PIQUE, A., GUERREIRO, P., MARIJANOVIC, Z., MENDES, T., RAMALHO, J., EMMANOUILIDOU, E., VENTURA, S., KLUCKEN, J., BARRAL, D. C., GIORGINI, F., VEKRELLIS, K. & OUTEIRO, T. F. 2014. The small GTPase Rab11 co-localizes with alpha-synuclein in intracellular inclusions and modulates its aggregation, secretion and toxicity. *Hum Mol Genet,* 23**,** 6732-45.

COOK, D. A., KANNARKAT, G. T., CINTRON, A. F., BUTKOVICH, L. M., FRASER, K. B., CHANG, J., GRIGORYAN, N., FACTOR, S. A., WEST, A. B., BOSS, J. M. & TANSEY, M. G. 2017. LRRK2 levels in immune cells are increased in Parkinson's disease. *NPJ Parkinsons Dis,* 3**,** 11.

COPPOLA, U., ANNONA, G., D'ANIELLO, S. & RISTORATORE, F. 2016. Rab32 and Rab38 genes in chordate pigmentation: an evolutionary perspective. *BMC Evol Biol,* 16**,** 26.

CORDING, A. C., SHIAELIS, N., PETRIDI, S., MIDDLETON, C. A., WILSON, L. G. & ELLIOTT, C. J. H. 2017. Targeted kinase inhibition relieves slowness and tremor in a Drosophila model of LRRK2 Parkinson's disease. *NPJ Parkinsons Dis,* 3**,** 34.

DAHANUKAR, A., LEI, Y. T., KWON, J. Y. & CARLSON, J. R. 2007. Two Gr genes underlie sugar reception in Drosophila. *Neuron,* 56**,** 503-16.

DAHER, J. P., PLETNIKOVA, O., BISKUP, S., MUSSO, A., GELLHAAR, S., GALTER, D., TRONCOSO, J. C., LEE, M. K., DAWSON, T. M., DAWSON, V. L. & MOORE, D. J. 2012. Neurodegenerative phenotypes in an A53T alpha-synuclein transgenic mouse model are independent of LRRK2. *Hum Mol Genet,* 21**,** 2420-31.

DAWSON, T. M., KO, H. S. & DAWSON, V. L. 2010. Genetic animal models of Parkinson's disease. *Neuron,* 66**,** 646-61.

DE LAU, L. M. & BRETELER, M. M. 2006. Epidemiology of Parkinson's disease. *Lancet Neurol,* 5**,** 525-35.

DHEKNE, H. S., YANATORI, I., GOMEZ, R. C., TONELLI, F., DIEZ, F., SCHULE, B., STEGER, M., ALESSI, D. R. & PFEFFER, S. R. 2018. A pathway for Parkinson's Disease LRRK2 kinase to block primary cilia and Sonic hedgehog signaling in the brain. *Elife,* 7.

DI MAIO, R., HOFFMAN, E. K., ROCHA, E. M., KEENEY, M. T., SANDERS, L. H., DE MIRANDA, B. R., ZHARIKOV, A., VAN LAAR, A., STEPAN, A. F., LANZ, T. A., KOFLER, J. K., BURTON, E. A., ALESSI, D. R., HASTINGS, T. G. & GREENAMYRE, J. T. 2018. LRRK2 activation in idiopathic Parkinson's disease. *Sci Transl Med,* 10.

DIRAC-SVEJSTRUP, A. B., SUMIZAWA, T. & PFEFFER, S. R. 1997. Identification of a GDI displacement factor that releases endosomal Rab GTPases from Rab-GDI. *EMBO J,* 16**,** 465-72.

EGUCHI, T., KUWAHARA, T., SAKURAI, M., KOMORI, T., FUJIMOTO, T., ITO, G., YOSHIMURA, S. I., HARADA, A., FUKUDA, M., KOIKE, M. & IWATSUBO, T. 2018. LRRK2 and its substrate Rab GTPases are sequentially targeted onto stressed lysosomes and maintain their homeostasis. *Proc Natl Acad Sci U S A,* 115**,** E9115-E9124.

FAN, Y., HOWDEN, A. J. M., SARHAN, A. R., LIS, P., ITO, G., MARTINEZ, T. N., BROCKMANN, K., GASSER, T., ALESSI, D. R. & SAMMLER, E. M. 2018. Interrogating Parkinson's disease LRRK2 kinase pathway activity by assessing Rab10 phosphorylation in human neutrophils. *Biochem J,* 475**,** 23-44.

FRIGGI-GRELIN, F., COULOM, H., MELLER, M., GOMEZ, D., HIRSH, J. & BIRMAN, S. 2003. Targeted gene expression in Drosophila dopaminergic cells using regulatory sequences from tyrosine hydroxylase. *J Neurobiol,* 54**,** 618-27.

FUJI, R. N., FLAGELLA, M., BACA, M., BAPTISTA, M. A., BRODBECK, J., CHAN, B. K., FISKE, B. K., HONIGBERG, L., JUBB, A. M., KATAVOLOS, P., LEE, D. W., LEWIN-KOH, S. C., LIN, T., LIU, X., LIU, S., LYSSIKATOS, J. P., O'MAHONY, J., REICHELT, M., ROOSE-GIRMA, M., SHENG, Z., SHERER, T., SMITH, A., SOLON, M., SWEENEY, Z. K., TARRANT, J., URKOWITZ, A., WARMING, S., YAYLAOGLU, M., ZHANG, S., ZHU, H., ESTRADA, A. A. & WATTS, R. J. 2015. Effect of selective LRRK2 kinase inhibition on nonhuman primate lung. *Sci Transl Med,* 7**,** 273ra15.

FUNAYAMA, M., HASEGAWA, K., KOWA, H., SAITO, M., TSUJI, S. & OBATA, F. 2002. A new locus for Parkinson's disease (PARK8) maps to chromosome 12p11.2-q13.1. *Ann Neurol,* 51**,** 296-301.

FUNG, H. C., SCHOLZ, S., MATARIN, M., SIMON-SANCHEZ, J., HERNANDEZ, D., BRITTON, A., GIBBS, J. R., LANGEFELD, C., STIEGERT, M. L., SCHYMICK, J., OKUN, M. S., MANDEL, R. J., FERNANDEZ, H. H., FOOTE, K. D., RODRIGUEZ, R. L., PECKHAM, E., DE VRIEZE, F. W., GWINN-HARDY, K., HARDY, J. A. & SINGLETON, A. 2006. Genome-wide genotyping in Parkinson's disease and neurologically normal controls: first stage analysis and public release of data. *Lancet Neurol,* 5**,** 911-6.

GALATSIS, P. 2017. Leucine-rich repeat kinase 2 inhibitors: a patent review (2014-2016). *Expert Opin Ther Pat,* 27**,** 667-676.

GIASSON, B. I., COVY, J. P., BONINI, N. M., HURTIG, H. I., FARRER, M. J., TROJANOWSKI, J. Q. & VAN DEERLIN, V. M. 2006. Biochemical and pathological characterization of Lrrk2. *Ann Neurol,* 59**,** 315-22.

GONZALEZ-REYES, L. E., VERBITSKY, M., BLESA, J., JACKSON-LEWIS, V., PAREDES, D., TILLACK, K., PHANI, S., KRAMER, E. R., PRZEDBORSKI, S. & KOTTMANN, A. H. 2012. Sonic hedgehog maintains cellular and neurochemical homeostasis in the adult nigrostriatal circuit. *Neuron,* 75**,** 306-19.

GORDON, M. D. & SCOTT, K. 2009. Motor control in a Drosophila taste circuit. *Neuron,* 61**,** 373-84.
GOSWAMI, J. N., SANKHYAN, N. & SINGHI, P. D. 2017. An Indian Family with Tyrosine Hydroxylase Deficiency. *Indian Pediatr,* 54**,** 499-501.
GUERREIRO, P. S., HUANG, Y., GYSBERS, A., CHENG, D., GAI, W. P., OUTEIRO, T. F. & HALLIDAY, G. M. 2013. LRRK2 interactions with alpha-synuclein in Parkinson's disease brains and in cell models. *J Mol Med (Berl),* 91**,** 513-22.
HARTENSTEIN, V., CRUZ, L., LOVICK, J. K. & GUO, M. 2017. Developmental analysis of the dopamine-containing neurons of the Drosophila brain. *J Comp Neurol,* 525**,** 363-379.
HASEGAWA, K., STOESSL, A. J., YOKOYAMA, T., KOWA, H., WSZOLEK, Z. K. & YAGISHITA, S. 2009. Familial parkinsonism: study of original Sagamihara PARK8 (I2020T) kindred with variable clinicopathologic outcomes. *Parkinsonism Relat Disord,* 15**,** 300-6.
HEALY, D. G., FALCHI, M., O'SULLIVAN, S. S., BONIFATI, V., DURR, A., BRESSMAN, S., BRICE, A., AASLY, J., ZABETIAN, C. P., GOLDWURM, S., FERREIRA, J. J., TOLOSA, E., KAY, D. M., KLEIN, C., WILLIAMS, D. R., MARRAS, C., LANG, A. E., WSZOLEK, Z. K., BERCIANO, J., SCHAPIRA, A. H., LYNCH, T., BHATIA, K. P., GASSER, T., LEES, A. J., WOOD, N. W. & INTERNATIONAL, L. C. 2008a. Phenotype, genotype, and worldwide genetic penetrance of LRRK2-associated Parkinson's disease: a case-control study. *Lancet Neurol,* 7**,** 583-90.
HEALY, D. G., WOOD, N. W. & SCHAPIRA, A. H. 2008b. Test for LRRK2 mutations in patients with Parkinson's disease. *Pract Neurol,* 8**,** 381-5.
HERBST, S. & GUTIERREZ, M. G. 2019. LRRK2 in Infection: Friend or Foe? *ACS Infect Dis,* 5**,** 809-815.
HIMMELBERG, M. M., WEST, R. J. H., WADE, A. R. & ELLIOTT, C. J. H. 2018. A perceptive plus in Parkinson's disease. *Mov Disord,* 33**,** 248.
HINDLE, S., AFSARI, F., STARK, M., MIDDLETON, C. A., EVANS, G. J., SWEENEY, S. T. & ELLIOTT, C. J. 2013. Dopaminergic expression of the Parkinsonian gene LRRK2-G2019S leads to non-autonomous visual neurodegeneration, accelerated by increased neural demands for energy. *Hum Mol Genet,* 22**,** 2129-40.
HOMMA, Y. & FUKUDA, M. 2016. Rabin8 regulates neurite outgrowth in both GEF activity-dependent and -independent manners. *Mol Biol Cell,* 27**,** 2107-18.
HOULDEN, H. & SINGLETON, A. B. 2012. The genetics and neuropathology of Parkinson's disease. *Acta Neuropathol,* 124**,** 325-38.
INAGAKI, H. K., JUNG, Y., HOOPFER, E. D., WONG, A. M., MISHRA, N., LIN, J. Y., TSIEN, R. Y. & ANDERSON, D. J. 2014. Optogenetic control of Drosophila using a red-shifted channelrhodopsin reveals experience-dependent influences on courtship. *Nat Methods,* 11**,** 325-32.
ITO, G., KATSEMONOVA, K., TONELLI, F., LIS, P., BAPTISTA, M. A., SHPIRO, N., DUDDY, G., WILSON, S., HO, P. W., HO, S. L., REITH, A. D. & ALESSI, D. R. 2016. Phos-tag analysis of Rab10 phosphorylation by LRRK2: a powerful assay for assessing kinase function and inhibitors. *Biochem J,* 473**,** 2671-85.
JALDIN-FINCATI, J. R., PAVAROTTI, M., FRENDO-CUMBO, S., BILAN, P. J. & KLIP, A. 2017. Update on GLUT4 Vesicle Traffic: A Cornerstone of Insulin Action. *Trends Endocrinol Metab,* 28**,** 597-611.
JANKOVIC, J. 2008. Parkinson's disease and movement disorders: moving forward. *Lancet Neurol,* 7**,** 9-11.
JEONG, G. R., JANG, E. H., BAE, J. R., JUN, S., KANG, H. C., PARK, C. H., SHIN, J. H., YAMAMOTO, Y., TANAKA-YAMAMOTO, K., DAWSON, V. L., DAWSON, T. M., HUR, E. M. & LEE, B. D. 2018. Dysregulated phosphorylation of Rab GTPases by LRRK2 induces neurodegeneration. *Mol Neurodegener,* 13**,** 8.
KACHERGUS, J., MATA, I. F., HULIHAN, M., TAYLOR, J. P., LINCOLN, S., AASLY, J., GIBSON, J. M., ROSS, O. A., LYNCH, T., WILEY, J., PAYAMI, H., NUTT, J., MARAGANORE, D. M., CZYZEWSKI, K., STYCZYNSKA, M., WSZOLEK, Z. K., FARRER, M. J. & TOFT, M. 2005. Identification of a novel LRRK2 mutation linked to autosomal dominant parkinsonism: evidence of a common founder across European populations. *Am J Hum Genet,* 76**,** 672-80.

KAWAKAMI, F., YABATA, T., OHTA, E., MAEKAWA, T., SHIMADA, N., SUZUKI, M., MARUYAMA, H., ICHIKAWA, T. & OBATA, F. 2012. LRRK2 phosphorylates tubulin-associated tau but not the free molecule: LRRK2-mediated regulation of the tau-tubulin association and neurite outgrowth. *PLoS One,* 7**,** e30834.

KIRAL, F. R., KOHRS, F. E., JIN, E. J. & HIESINGER, P. R. 2018. Rab GTPases and Membrane Trafficking in Neurodegeneration. *Curr Biol,* 28**,** R471-R486.

KRUGER, R., KUHN, W., MULLER, T., WOITALLA, D., GRAEBER, M., KOSEL, S., PRZUNTEK, H., EPPLEN, J. T., SCHOLS, L. & RIESS, O. 1998. Ala30Pro mutation in the gene encoding alpha-synuclein in Parkinson's disease. *Nat Genet,* 18**,** 106-8.

LAI, S. L. & LEE, T. 2006. Genetic mosaic with dual binary transcriptional systems in Drosophila. *Nat Neurosci,* 9**,** 703-9.

LAI, Y. C., KONDAPALLI, C., LEHNECK, R., PROCTER, J. B., DILL, B. D., WOODROOF, H. I., GOURLAY, R., PEGGIE, M., MACARTNEY, T. J., CORTI, O., CORVOL, J. C., CAMPBELL, D. G., ITZEN, A., TROST, M. & MUQIT, M. M. 2015. Phosphoproteomic screening identifies Rab GTPases as novel downstream targets of PINK1. *EMBO J,* 34**,** 2840-61.

LARANCE, M., RAMM, G., STOCKLI, J., VAN DAM, E. M., WINATA, S., WASINGER, V., SIMPSON, F., GRAHAM, M., JUNUTULA, J. R., GUILHAUS, M. & JAMES, D. E. 2005. Characterization of the role of the Rab GTPase-activating protein AS160 in insulin-regulated GLUT4 trafficking. *J Biol Chem,* 280**,** 37803-13.

LAVALLEY, N. J., SLONE, S. R., DING, H., WEST, A. B. & YACOUBIAN, T. A. 2016. 14-3-3 Proteins regulate mutant LRRK2 kinase activity and neurite shortening. *Hum Mol Genet,* 25**,** 109-22.

LESAGE, S., LEUTENEGGER, A. L., IBANEZ, P., JANIN, S., LOHMANN, E., DURR, A., BRICE, A. & FRENCH PARKINSON'S DISEASE GENETICS STUDY, G. 2005. LRRK2 haplotype analyses in European and North African families with Parkinson disease: a common founder for the G2019S mutation dating from the 13th century. *Am J Hum Genet,* 77**,** 330-2.

LI, Z., SCHULZE, R. J., WELLER, S. G., KRUEGER, E. W., SCHOTT, M. B., ZHANG, X., CASEY, C. A., LIU, J., STOCKLI, J., JAMES, D. E. & MCNIVEN, M. A. 2016. A novel Rab10-EHBP1-EHD2 complex essential for the autophagic engulfment of lipid droplets. *Sci Adv,* 2**,** e1601470.

LIN, J. Y., KNUTSEN, P. M., MULLER, A., KLEINFELD, D. & TSIEN, R. Y. 2013. ReaChR: a red-shifted variant of channelrhodopsin enables deep transcranial optogenetic excitation. *Nat Neurosci,* 16**,** 1499-508.

LIN, X., PARISIADOU, L., GU, X. L., WANG, L., SHIM, H., SUN, L., XIE, C., LONG, C. X., YANG, W. J., DING, J., CHEN, Z. Z., GALLANT, P. E., TAO-CHENG, J. H., RUDOW, G., TRONCOSO, J. C., LIU, Z., LI, Z. & CAI, H. 2009. Leucine-rich repeat kinase 2 regulates the progression of neuropathology induced by Parkinson's-disease-related mutant alpha-synuclein. *Neuron,* 64**,** 807-27.

LIS, P., BUREL, S., STEGER, M., MANN, M., BROWN, F., DIEZ, F., TONELLI, F., HOLTON, J. L., HO, P. W., HO, S. L., CHOU, M. Y., POLINSKI, N. K., MARTINEZ, T. N., DAVIES, P. & ALESSI, D. R. 2018. Development of phospho-specific Rab protein antibodies to monitor in vivo activity of the LRRK2 Parkinson's disease kinase. *Biochem J,* 475**,** 1-22.

LIU, Z., WANG, X., YU, Y., LI, X., WANG, T., JIANG, H., REN, Q., JIAO, Y., SAWA, A., MORAN, T., ROSS, C. A., MONTELL, C. & SMITH, W. W. 2008. A Drosophila model for LRRK2-linked parkinsonism. *Proc Natl Acad Sci U S A,* 105**,** 2693-8.

LYND, A. & LYCETT, G. J. 2011. Optimization of the Gal4-UAS system in an Anopheles gambiae cell line. *Insect Mol Biol,* 20**,** 599-608.

MACLEOD, D. A., RHINN, H., KUWAHARA, T., ZOLIN, A., DI PAOLO, G., MCCABE, B. D., MARDER, K. S., HONIG, L. S., CLARK, L. N., SMALL, S. A. & ABELIOVICH, A. 2013. RAB7L1 interacts with LRRK2 to modify intraneuronal protein sorting and Parkinson's disease risk. *Neuron,* 77**,** 425-39.

MARAGANORE, D. M., DE ANDRADE, M., ELBAZ, A., FARRER, M. J., IOANNIDIS, J. P., KRUGER, R., ROCCA, W. A., SCHNEIDER, N. K., LESNICK, T. G., LINCOLN, S. J., HULIHAN, M. M., AASLY, J. O., ASHIZAWA, T., CHARTIER-HARLIN, M. C., CHECKOWAY, H., FERRARESE, C., HADJIGEORGIOU, G., HATTORI, N., KAWAKAMI, H., LAMBERT, J. C., LYNCH, T., MELLICK, G. D.,

PAPAPETROPOULOS, S., PARSIAN, A., QUATTRONE, A., RIESS, O., TAN, E. K., VAN BROECKHOVEN, C. & GENETIC EPIDEMIOLOGY OF PARKINSON'S DISEASE, C. 2006. Collaborative analysis of alpha-synuclein gene promoter variability and Parkinson disease. *JAMA,* 296**,** 661-70.

MARELLA, S., MANN, K. & SCOTT, K. 2012. Dopaminergic modulation of sucrose acceptance behavior in Drosophila. *Neuron,* 73**,** 941-50.

MARSDEN, C. D. 1961. Pigmentation in the nucleus substantiae nigrae of mammals. *J Anat,* 95**,** 256-61.

MARSH, L. 2013. Depression and Parkinson's disease: current knowledge. *Curr Neurol Neurosci Rep,* 13**,** 409.

MARTI-MASSO, J. F., RUIZ-MARTINEZ, J., BOLANO, M. J., RUIZ, I., GOROSTIDI, A., MORENO, F., FERRER, I. & LOPEZ DE MUNAIN, A. 2009. Neuropathology of Parkinson's disease with the R1441G mutation in LRRK2. *Mov Disord,* 24**,** 1998-2001.

MATA, I. F., KACHERGUS, J. M., TAYLOR, J. P., LINCOLN, S., AASLY, J., LYNCH, T., HULIHAN, M. M., COBB, S. A., WU, R. M., LU, C. S., LAHOZ, C., WSZOLEK, Z. K. & FARRER, M. J. 2005. Lrrk2 pathogenic substitutions in Parkinson's disease. *Neurogenetics,* 6**,** 171-7.

MIR, R., TONELLI, F., LIS, P., MACARTNEY, T., POLINSKI, N. K., MARTINEZ, T. N., CHOU, M. Y., HOWDEN, A. J. M., KONIG, T., HOTZY, C., MILENKOVIC, I., BRUCKE, T., ZIMPRICH, A., SAMMLER, E. & ALESSI, D. R. 2018. The Parkinson's disease VPS35[D620N] mutation enhances LRRK2-mediated Rab protein phosphorylation in mouse and human. *Biochem J,* 475**,** 1861-1883.

NICHOLS, W. C., PANKRATZ, N., HERNANDEZ, D., PAISAN-RUIZ, C., JAIN, S., HALTER, C. A., MICHAELS, V. E., REED, T., RUDOLPH, A., SHULTS, C. W., SINGLETON, A., FOROUD, T. & PARKINSON STUDY GROUP, P. I. 2005. Genetic screening for a single common LRRK2 mutation in familial Parkinson's disease. *Lancet,* 365**,** 410-2.

PEREIRA-LEAL, J. B. & SEABRA, M. C. 2000. The mammalian Rab family of small GTPases: definition of family and subfamily sequence motifs suggests a mechanism for functional specificity in the Ras superfamily. *J Mol Biol,* 301**,** 1077-87.

POLYMEROPOULOS, M. H., HURKO, O., HSU, F., RUBENSTEIN, J., BASNET, S., LANE, K., DIETZ, H., SPETZLER, R. F. & RIGAMONTI, D. 1997. Linkage of the locus for cerebral cavernous hemangiomas to human chromosome 7q in four families of Mexican-American descent. *Neurology,* 48**,** 752-7.

POWER, J. H., BARNES, O. L. & CHEGINI, F. 2017. Lewy Bodies and the Mechanisms of Neuronal Cell Death in Parkinson's Disease and Dementia with Lewy Bodies. *Brain Pathol,* 27**,** 3-12.

PROGIDA, C. & BAKKE, O. 2016. Bidirectional traffic between the Golgi and the endosomes - machineries and regulation. *J Cell Sci,* 129**,** 3971-3982.

PURLYTE, E., DHEKNE, H. S., SARHAN, A. R., GOMEZ, R., LIS, P., WIGHTMAN, M., MARTINEZ, T. N., TONELLI, F., PFEFFER, S. R. & ALESSI, D. R. 2018. Rab29 activation of the Parkinson's disease-associated LRRK2 kinase. *EMBO J,* 37**,** 1-18.

PYLYPENKO, O., HAMMICH, H., YU, I. M. & HOUDUSSE, A. 2018. Rab GTPases and their interacting protein partners: Structural insights into Rab functional diversity. *Small GTPases,* 9**,** 22-48.

REED, X., BANDRES-CIGA, S., BLAUWENDRAAT, C. & COOKSON, M. R. 2018. The role of monogenic genes in idiopathic Parkinson's disease. *Neurobiol Dis,* 124**,** 230-239.

REITER, L. T., POTOCKI, L., CHIEN, S., GRIBSKOV, M. & BIER, E. 2001. A systematic analysis of human disease-associated gene sequences in Drosophila melanogaster. *Genome Res,* 11**,** 1114-25.

SADOWSKI, I., MA, J., TRIEZENBERG, S. & PTASHNE, M. 1988. GAL4-VP16 is an unusually potent transcriptional activator. *Nature,* 335**,** 563-4.

SATO, T., IWANO, T., KUNII, M., MATSUDA, S., MIZUGUCHI, R., JUNG, Y., HAGIWARA, H., YOSHIHARA, Y., YUZAKI, M., HARADA, R. & HARADA, A. 2014. Rab8a and Rab8b are essential for several apical transport pathways but insufficient for ciliogenesis. *J Cell Sci,* 127**,** 422-31.

SCHAUB, J. R. & STEARNS, T. 2013. The Rilp-like proteins Rilpl1 and Rilpl2 regulate ciliary membrane content. *Mol Biol Cell,* 24**,** 453-64.

SHANLEY, M. R., HAWLEY, D., LEUNG, S., ZAIDI, N. F., DAVE, R., SCHLOSSER, K. A., BANDOPADHYAY, R., GERBER, S. A. & LIU, M. 2015. LRRK2 Facilitates tau Phosphorylation through Strong Interaction with tau and cdk5. *Biochemistry,* 54**,** 5198-208.

SINGLETON, A. B., FARRER, M., JOHNSON, J., SINGLETON, A., HAGUE, S., KACHERGUS, J., HULIHAN, M., PEURALINNA, T., DUTRA, A., NUSSBAUM, R., LINCOLN, S., CRAWLEY, A., HANSON, M., MARAGANORE, D., ADLER, C., COOKSON, M. R., MUENTER, M., BAPTISTA, M., MILLER, D., BLANCATO, J., HARDY, J. & GWINN-HARDY, K. 2003. alpha-Synuclein locus triplication causes Parkinson's disease. *Science,* 302**,** 841.

SPILLANTINI, M. G., SCHMIDT, M. L., LEE, V. M., TROJANOWSKI, J. Q., JAKES, R. & GOEDERT, M. 1997. Alpha-synuclein in Lewy bodies. *Nature,* 388**,** 839-40.

STEGER, M., DIEZ, F., DHEKNE, H. S., LIS, P., NIRUJOGI, R. S., KARAYEL, O., TONELLI, F., MARTINEZ, T. N., LORENTZEN, E., PFEFFER, S. R., ALESSI, D. R. & MANN, M. 2017. Systematic proteomic analysis of LRRK2-mediated Rab GTPase phosphorylation establishes a connection to ciliogenesis. *Elife,* 6.

STEGER, M., TONELLI, F., ITO, G., DAVIES, P., TROST, M., VETTER, M., WACHTER, S., LORENTZEN, E., DUDDY, G., WILSON, S., BAPTISTA, M. A., FISKE, B. K., FELL, M. J., MORROW, J. A., REITH, A. D., ALESSI, D. R. & MANN, M. 2016. Phosphoproteomics reveals that Parkinson's disease kinase LRRK2 regulates a subset of Rab GTPases. *Elife,* 5.

TAVANA, J. P., ROSENE, M., JENSEN, N. O., RIDGE, P. G., KAUWE, J. S. & KARCH, C. M. 2019. RAB10: an Alzheimer's disease resilience locus and potential drug target. *Clin Interv Aging,* 14**,** 73-79.

TOMKINS, J. E., DIHANICH, S., BEILINA, A., FERRARI, R., ILACQUA, N., COOKSON, M. R., LEWIS, P. A. & MANZONI, C. 2018. Comparative Protein Interaction Network Analysis Identifies Shared and Distinct Functions for the Human ROCO Proteins. *Proteomics,* 18**,** e1700444.

TWIG, G. & SHIRIHAI, O. S. 2011. The interplay between mitochondrial dynamics and mitophagy. *Antioxid Redox Signal,* 14**,** 1939-51.

UDAYAR, V., BUGGIA-PREVOT, V., GUERREIRO, R. L., SIEGEL, G., RAMBABU, N., SOOHOO, A. L., PONNUSAMY, M., SIEGENTHALER, B., BALI, J., AESG, SIMONS, M., RIES, J., PUTHENVEEDU, M. A., HARDY, J., THINAKARAN, G. & RAJENDRAN, L. 2013. A paired RNAi and RabGAP overexpression screen identifies Rab11 as a regulator of beta-amyloid production. *Cell Rep,* 5**,** 1536-51.

UJIIE, S., HATANO, T., KUBO, S., IMAI, S., SATO, S., UCHIHARA, T., YAGISHITA, S., HASEGAWA, K., KOWA, H., SAKAI, F. & HATTORI, N. 2012. LRRK2 I2020T mutation is associated with tau pathology. *Parkinsonism Relat Disord,* 18**,** 819-23.

ULMER, T. S., BAX, A., COLE, N. B. & NUSSBAUM, R. L. 2005. Structure and dynamics of micelle-bound human alpha-synuclein. *J Biol Chem,* 280**,** 9595-603.

VETTER, I. R. & WITTINGHOFER, A. 2001. The guanine nucleotide-binding switch in three dimensions. *Science,* 294**,** 1299-304.

VILARINO-GUELL, C., WIDER, C., ROSS, O. A., DACHSEL, J. C., KACHERGUS, J. M., LINCOLN, S. J., SOTO-ORTOLAZA, A. I., COBB, S. A., WILHOITE, G. J., BACON, J. A., BEHROUZ, B., MELROSE, H. L., HENTATI, E., PUSCHMANN, A., EVANS, D. M., CONIBEAR, E., WASSERMAN, W. W., AASLY, J. O., BURKHARD, P. R., DJALDETTI, R., GHIKA, J., HENTATI, F., KRYGOWSKA-WAJS, A., LYNCH, T., MELAMED, E., RAJPUT, A., RAJPUT, A. H., SOLIDA, A., WU, R. M., UITTI, R. J., WSZOLEK, Z. K., VINGERHOETS, F. & FARRER, M. J. 2011. VPS35 mutations in Parkinson disease. *Am J Hum Genet,* 89**,** 162-7.

WAUTERS, F., CORNELISSEN, T., IMBERECHTS, D., MARTIN, S., KOENTJORO, B., SUE, C., VANGHELUWE, P. & VANDENBERGHE, W. 2019. LRRK2 mutations impair depolarization-induced mitophagy through inhibition of mitochondrial accumulation of RAB10. *Autophagy***,** 1-20.

WEIL, R., LAPLANTINE, E., CURIC, S. & GENIN, P. 2018. Role of Optineurin in the Mitochondrial Dysfunction: Potential Implications in Neurodegenerative Diseases and Cancer. *Front Immunol,* 9**,** 1243.

WEST, A. B., MOORE, D. J., BISKUP, S., BUGAYENKO, A., SMITH, W. W., ROSS, C. A., DAWSON, V. L. & DAWSON, T. M. 2005. Parkinson's disease-associated mutations in leucine-rich repeat kinase 2 augment kinase activity. *Proc Natl Acad Sci U S A,* 102**,** 16842-7.

WHITWORTH, A. J. 2011. Drosophila models of Parkinson's disease. *Adv Genet,* 73**,** 1-50.

WRAY, S. & LEWIS, P. A. 2010. A tangled web - tau and sporadic Parkinson's disease. *Front Psychiatry,* 1**,** 150.

YAN, T., WANG, L., GAO, J., SIEDLAK, S. L., HUNTLEY, M. L., TERMSARASAB, P., PERRY, G., CHEN, S. G. & WANG, X. 2018. Rab10 Phosphorylation is a Prominent Pathological Feature in Alzheimer's Disease. *J Alzheimers Dis,* 63**,** 157-165.

YOSHIZAKI, T., IMAMURA, T., BABENDURE, J. L., LU, J. C., SONODA, N. & OLEFSKY, J. M. 2007. Myosin 5a is an insulin-stimulated Akt2 (protein kinase Bbeta) substrate modulating GLUT4 vesicle translocation. *Mol Cell Biol,* 27**,** 5172-83.

ZARRANZ, J. J., ALEGRE, J., GOMEZ-ESTEBAN, J. C., LEZCANO, E., ROS, R., AMPUERO, I., VIDAL, L., HOENICKA, J., RODRIGUEZ, O., ATARES, B., LLORENS, V., GOMEZ TORTOSA, E., DEL SER, T., MUNOZ, D. G. & DE YEBENES, J. G. 2004. The new mutation, E46K, of alpha-synuclein causes Parkinson and Lewy body dementia. *Ann Neurol,* 55**,** 164-73.

ZHANG, H., DUAN, C. & YANG, H. 2015. Defective autophagy in Parkinson's disease: lessons from genetics. *Mol Neurobiol,* 51**,** 89-104.

ZHANG, J., SCHULZE, K. L., HIESINGER, P. R., SUYAMA, K., WANG, S., FISH, M., ACAR, M., HOSKINS, R. A., BELLEN, H. J. & SCOTT, M. P. 2007. Thirty-one flavors of Drosophila rab proteins. *Genetics,* 176**,** 1307-22.

ZHANG, X., GAO, F., WANG, D., LI, C., FU, Y., HE, W. & ZHANG, J. 2018. Tau Pathology in Parkinson's Disease. *Front Neurol,* 9**,** 809.

ZHEN, Y. & STENMARK, H. 2015. Cellular functions of Rab GTPases at a glance. *J Cell Sci,* 128**,** 3171-6.